



## Ultrasonic P- and S-Wave Attenuation and Petrophysical Properties of Deccan Flood Basalts, India, as Revealed by Borehole Studies

NIMISHA VEDANTI,<sup>1,2</sup> AJAY MALKOTI,<sup>1,2</sup> O. P. PANDEY,<sup>1</sup> and J. P. SHRIVASTAVA<sup>3</sup>

**Abstract**—Petrophysical properties and ultrasonic P- and S-wave attenuation measurements on 35 Deccan basalt core specimens, recovered from Killari borehole site in western India, provide unique reference data-sets for a lesser studied Deccan Volcanic Province. These samples represent 338-m-thick basaltic column, consisting four lava flows each of Ambenali and Poladpur Formations, belonging to Wai Subgroup of the Deccan volcanic sequence. These basalt samples are found to be iron-rich (average  $\text{FeO}_T$ : 13.4 wt%), but relatively poor in silica content (average  $\text{SiO}_2$ : 47.8 wt%). The saturated massive basalt cores are characterized by a mean density of  $2.91 \text{ g/cm}^3$  (range  $2.80\text{--}3.01 \text{ g/cm}^3$ ) and mean P- and S-wave velocities of  $5.89 \text{ km/s}$  (range  $5.01\text{--}6.50 \text{ km/s}$ ) and  $3.43 \text{ km/s}$  (range  $2.84\text{--}3.69 \text{ km/s}$ ), respectively. In comparison, saturated vesicular basalt cores show a wide range in density ( $2.40\text{--}2.79 \text{ g/cm}^3$ ) as well as P-wave ( $3.28\text{--}4.78 \text{ km/s}$ ) and S-wave ( $1.70\text{--}2.95 \text{ km/s}$ ) velocities. Based on the present study, the Deccan volcanic sequence can be assigned a weighted mean density of  $2.74 \text{ g/cm}^3$  and a low  $V_p$  and  $V_s$  of  $5.00$  and  $3.00 \text{ km/s}$ , respectively. Such low velocities in Deccan basalts can be attributed mainly to the presence of fine-grained glassy material, high iron contents, and hydrothermally altered secondary mineral products, besides higher porosity in vesicular samples. The measured Q values in saturated massive basalt cores vary enormously ( $Q_p$ : 33–1960 and  $Q_s$ : 35–506), while saturated vesicular basalt samples exhibit somewhat lesser variation in  $Q_p$  (6–46) as well as  $Q_s$  (5–49). In general, high-porosity rocks exhibit high attenuation, but we observed the high value of attenuation in some of the massive basalt core samples also. In such cases, energy loss is mainly due to the presence of fine-grained glassy material as well as secondary alteration products like chlorophaeite, that could contribute to intrinsic attenuation. Dominance of weakly bound secondary minerals might also be responsible for the generation of microcracks, which may generate squirt flow in saturated samples. Hence, we argue that the Deccan basalts attenuate seismic energy significantly, where its composition plays a major role.

**Key words:** Petrophysical properties, P- and S-wave attenuation, massive and vesicular basalts, Ambenali and Poladpur Formations, Killari borehole, Deccan traps.

### 1. Introduction

The Deccan Volcanic Province, covered by a thick suite of 66-Ma-old basaltic lavas, forms one of the prominent large igneous provinces (LIP) on the surface of the earth (Fig. 1). It covers almost 1/6 of the Indian landmass around western margin and central part of India. This region has been seismically active since historical times, having experienced a number of damaging earthquakes in the past (Pandey 2009) that includes, 1993 Killari earthquake ( $M_w$  6.3) which took place in eastern region of Maharashtra and caused unprecedented damage to human lives and properties (Pandey et al. 2009; Gupta et al. 1993). Almost 10,000 people were killed by this deadly earthquake.

To study the seismotectonics of this earthquake-prone province in general and Killari earthquake region in particular, several boreholes were drilled in and around epicentral area. This included the 617-m-deep KLR-1 borehole, drilled 80 m south of surface scarp on the hanging wall near the Killari village ( $18^\circ 03' 07'' \text{N}$ ,  $76^\circ 33' 20'' \text{E}$ ) (Gupta et al. 2003). It was drilled by Atomic Minerals Directorate (AMD) and CSIR-National Geophysical Research Institute, Hyderabad (CSIR-NGRI) (Gupta and Dwivedi 1996). The borehole penetrated 338-m-thick basalt flows, followed by 8 m of infratrappean sediments and a further 270 m of the Neoarchean crystalline basement. The borehole was fully cored.

<sup>1</sup> CSIR-National Geophysical Research Institute, Uppal Road, Hyderabad 500007, India. E-mail: om\_pandey@rediffmail.com

<sup>2</sup> Academy for Scientific and Innovative Research (AcSIR), CSIR-NGRI, Uppal Road, Hyderabad 500007, India.

<sup>3</sup> Department of Geology, University of Delhi, Delhi 110007, India.

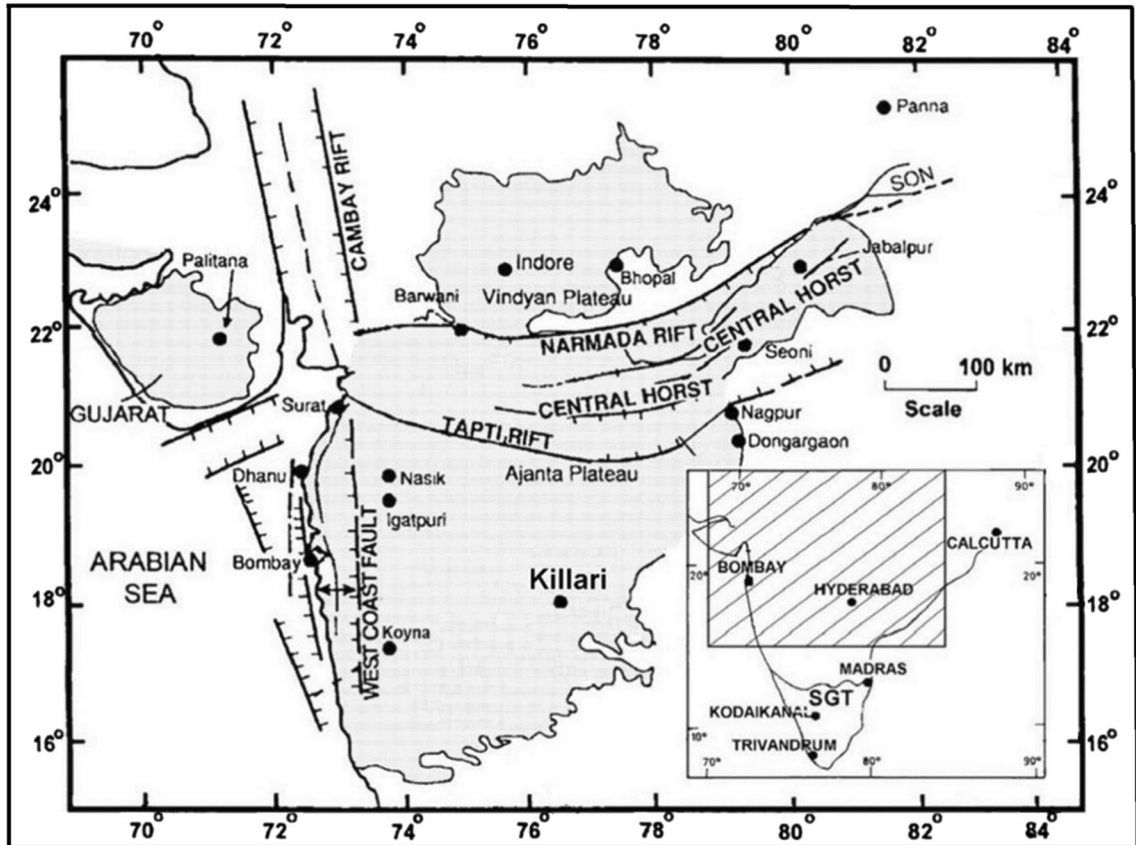


Figure 1

Tectonic map of the part of the Peninsular India, showing location of Killari and major rift valleys. Area covered by Deccan volcanics are shaded. SGT refers to Southern Granulite Terrain

Detailed geoscientific studies (including seismic, elastic and petrophysical studies) on the representative basement cores indicated the Neoarchean crystalline crust to be made up of high-density, high-velocity, metasomatized and exhumed amphibolite to granulite facies rocks, having mid-crustal characteristics (Pandey et al. 2009, 2014, 2016; Pandey 2016; Tripathi et al. 2012a, b; Tripathi 2015). However, very little study has been undertaken on the volcanic sequence that overlies the crystalline basement, except for the density (Gupta et al. 2003). In fact, no seismic attenuation study has yet been undertaken on Deccan basalt cores, apart from Weiner et al. (1987) who studied ultrasonic P- and S-wave attenuation characteristics and estimated  $Q_p$  for two tholeiitic basalts from Deccan Traps, using the torsional pendulum technique. Their measurements, at very low

frequencies (1.3 Hz), produced  $Q_s$  (shear wave quality factor) values ranging from 25 to  $> 1000$ , which was similar to that determined by Volarovitch and Gurvitch (1957) for basalt samples from USSR. Weiner et al. (1987) concluded that viscous sliding at grain boundaries causes relaxation and anelastic energy loss in the core samples. In view of the paucity of such data, an attempt has been made here to investigate ultrasonic P- and S-wave attenuation and petrophysical properties along with their geological characteristics on 35 chosen basalt core specimens that provide a new reference data set on Deccan basalts. Present work offers a new insight into the mechanism responsible for observed seismic wave energy loss in basalts. Such information is crucial for the seismic modeling of the sub-basalt formations, as well as underlying deep structural features.

## 2. Regional Geology

The Deccan volcanic sequence covers almost half a million sq. km on both onshore and offshore, across the west coast of India and consists of a number of gently dipping basalt flows with a cumulative thickness exceeding 2 km in Western Ghat section that parallels the west coast. These flows are highly differentiated, partially eroded at the surface and characterized mainly by tholeiitic composition. The major portion of these volcanics seems to have erupted in a quick succession during less than one million years (Courtillot et al. 1988; Renne et al. 2015) across Cretaceous–Paleocene (K/Pb) boundary dated 66 Ma (Gradstein et al. 2012), although some of the lava flow sequences (like Mandla lavas) may be relatively younger ( $64.21 \pm 0.33$  Ma) than the main Deccan volcanic event (Shrivastava et al. 2014, 2015, 2017). Palaeomagnetic data put these formations in chron 29 R (Schoene et al. 2015).

Present study area is situated in the southern part of the Deccan volcanic cover in the state of Eastern Maharashtra (Fig. 1), where the volcanic sequence comprised mainly two prominent formations, Ambenali and Poladpur, belonging to the Wai Sub-group (Mitchell and Widdowson 1991; Jay and Widdowson 2008). Both of these formations make the thickest sequence in Western Deccan Trap region. 338-m-thick drilled sequence in KLR-1 borehole at Killari, consisted 8 different flows of aa-type (blocky lavas), having an amygdaloidal and/or vuggy top, a massive interior and chilled glassy basal part (Gupta et al. 2003). In some flows, pipe amygdalites are also observed between the quenched basal part and the massive central part (Gupta and Gupta 2003; Parthasarathy et al. 2003). Out of the eight flows, the first four flows lying above the red boles (encountered between 173 and 178 m depth), belong to Ambenali Formation, while the rest four flows at the bottom to Poladpur Formation. Initial density measurements carried out on the samples from the three boreholes KLR-1, 2, 3 (Reddy et al. 1998), indicated that the 53% of the volcanic sequence comprised massive variety and the rest 47%, vesicular and amygdaloidal (non-massive) variety. Mineralogical studies on secondary minerals from various vesicular sections of the KLR-1 borehole (Parthasarathy et al. 2003;

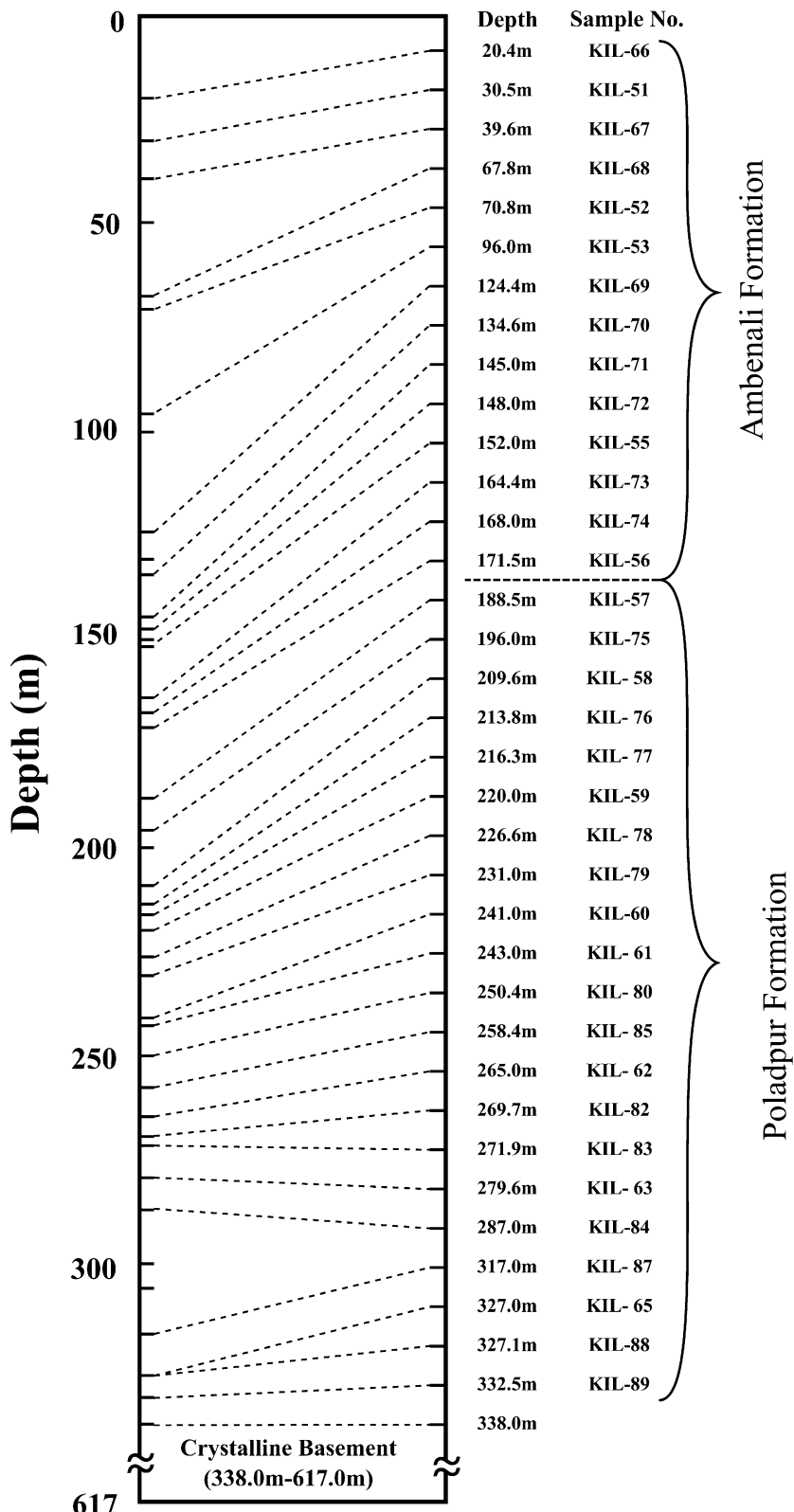
Parthasarathy 2006), indicated these to contain various forms of zeolites, calcite, chalcedony and clay minerals as amygdaloidal fillings, apart from moganite (a novel silica polymorph) and ferrous saponite.

## 3. Sample Description and Experimental Techniques

We choose 35 dry, compact and sufficiently homogeneous cores from the KLR-1 borehole, which are greenish black to dark shining black in luster. These belong to the depths ranging between 20.5 and 332.5 m (Fig. 2), thereby covering the entire column of the Ambenali and Poladpur volcanic formations, stacked over the Killari basement. Although our samples were in the form of compact cores, we obtained core plugs that are specially cut from the whole cores for pursuing elastic and petrophysical properties measurements. Special saws are used to cut these core plugs and their faces. All the samples were machined and polished so that their end faces were flat and parallel. Thus, these core plugs were in the form of right circular cylinders and had a constant diameter of 30 mm, but their length varied. This procedure was necessary in order to accurately measure the bulk volume using the physical dimensions of the sample, as well as to ensure good coupling between the interfaces and the transducers. Since the rock property experiments are more appropriate under saturated conditions, we saturated the samples in distilled water under vacuum to represent near-field conditions. All the measurements were made both in dry as well as saturated states and at room temperature/pressure conditions in Rock Mechanics Laboratory of CSIR-NGRI, Hyderabad (India) following standard procedures, recommended by the International Society for Rock Mechanics (Brown 1981).

### 3.1. Density and Porosity

Estimation of the density and porosity involves measurement of the bulk volume of the sample, which is mostly done either by fluid displacement (or volumetric) method or by the direct calculation. Measurements by fluid displacement method involves



**◀Figure 2**

Depths of the analyzed Deccan basalt samples from the KLR-1 borehole, drilled in the epicentral zone of 1993 Killari earthquake, Maharashtra India. Samples above 173 m belong to Ambenali Formation and below this depth, to Poladpur Formation. Positions of the samples are shown on left side and their corresponding number as well as depths, are shown on the right side

gravimetric (or Archimedes) method which is somewhat similar to the triple-weight method of porosity measurement, or alternatively, measurements through pycnometer. This method is commonly used for irregularly shaped samples; however, it is not suitable for vesicular samples which will absorb water.

In comparison, the direct method is preferred for regularly shaped cores (or core plugs) wherein the bulk volume can be accurately calculated using the physical dimensions of the perfectly cylindrical core samples, like the present case. For density measurements in the dry state, the samples were oven-dried at around 80 °C for about an hour in order to completely remove the moisture. Their diameter and length were repeatedly measured a few times using Vernier caliper, which has a precision of 0.02 mm. Their averages are then used for computing the bulk volume ( $v$ ). Similarly, the mass ( $m$ ) of each core was measured using an electronic balance with a precision of 0.001 g. The density ( $\rho$ ) of the specimen was obtained by using the formula,  $\rho = m/v$ .

Since the pore volume existing in the core samples can have an important bearing on petrophysical properties, we also measured the porosity. For this, we followed the water saturation method in which the mass of the core specimen is measured before and after the saturation of the samples. The difference in mass after and before saturation and the volume of the core specimen are then used for obtaining the porosity of specimens. The measured porosity can be considered as the effective porosity corresponding to connected pores within the specimen.

### 3.2. P- and S-Wave Velocity

The single directional velocity measurements were made both in dry and saturated states, following the standard method of time-of-flight ultrasonic pulse transmission technique, using the lab procedure described by Rao and Prasanna Lakshmi (2003), Rao

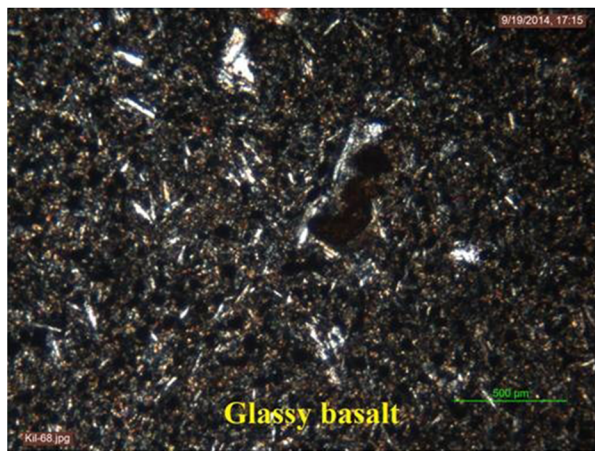
et al. (2006) and Prasanna Lakshmi et al. (2014). To facilitate the transmission of sound energy between the transducer and the test sample, the piezoelectric transducers were coupled to the specimen on both sides. A very thin film of the machine oil (for P-waves) and honey (for S-waves) was used as acoustic couplants between transducers and the sample to effectively facilitate the transmission of acoustic waves. This will ensure that there is no air between the transducers and the face of the core. Further, during the measurements, the transmitter is pressed to the center of a plane normal to the direction of wave propagation that would generate a stress of about 10 N/cm<sup>2</sup> (Brown 1981). Two different sets of transducers were used to measure  $V_p$  and  $V_s$ . Both, the transmitting and receiving transducers, were kept in a specially made housings having suitable damping material. A high energy pulser (Olympus Model No. 5058 PR) is used for generating electrical pulses. The transmitting transducer converts these electrical pulses into stress pulses that travel through the sample. At the receiving end, the stress pulses are converted into electrical pulses by the receiving transducer. The electric pulse is viewed using a 2-channel digital storage oscilloscope for travel time measurement. The arrival times of P- and S-waves are measured accurately with a precision of ± 1 and ± 2%, respectively, at 1 MHz frequency. The velocities are then calculated using the sample length and ultrasonic travel time in the studied core. Similar methods for velocity measurements have been in use worldwide (Birch 1960 and references therein; Ivankina et al. 2005; Ji et al. 2009; Kern et al. 2009). The main differences in such type of measurements are the frequencies, which normally vary from 1 to 2 MHz.

After measuring the velocities and taking into account the earlier measured density, we calculated the Poisson's ratio ( $\nu$ ) and Young's modulus ( $E$ ) using the relationships:

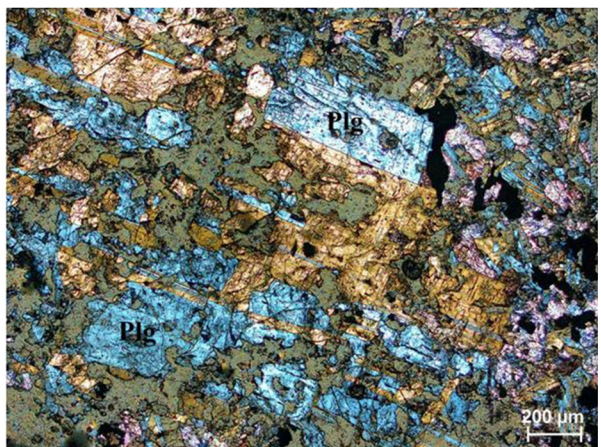
$$\text{Poisson's ratio, } \nu = \frac{1}{2} \left( \frac{V_p}{V_s} \right)^2 - 1$$

$$\text{Young's modulus, } E = \frac{\rho(1+\nu)(1-2\nu)V_p^2}{1+\nu}$$

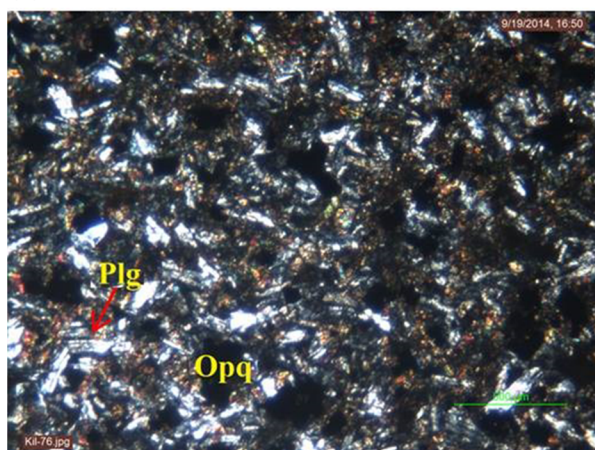
(a)



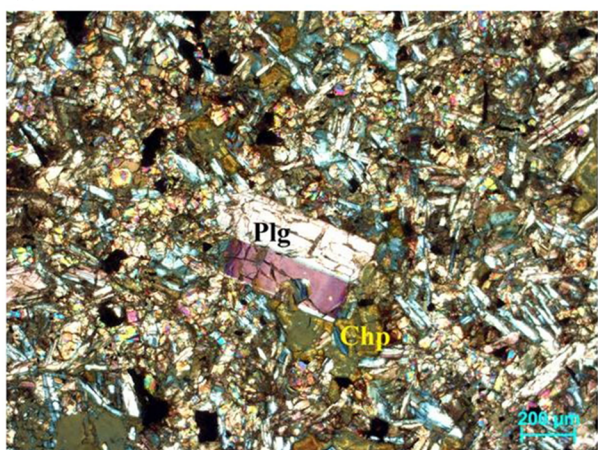
(d)



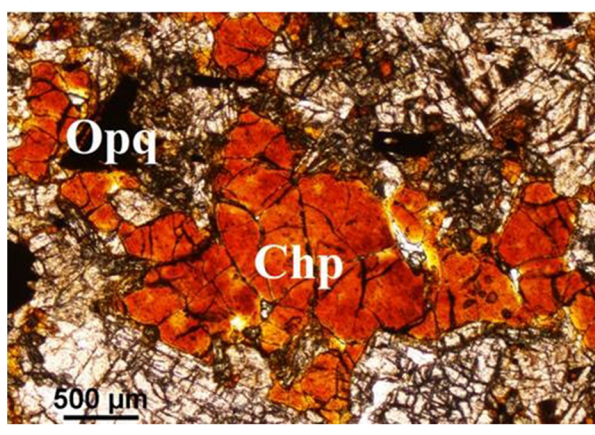
(b)



(e)



(c)



(f)



**◀Figure 3**

Photomicrographs taken from the thin sections of Deccan basalts showing glassy nature in sample KIL-68 (**a**), opaques and plagioclase laths in sample KIL 76 (**b**), chlorophaeite, opaques and plagioclase in sample KIL 87 (**c**), alteration of a big plagioclase grain into secondary minerals in KIL 74 (**d**), highly altered plagioclase grain and chlorophaeite in KIL 79 (**e**) and widespread alteration of plagioclase and pyroxene grains, as seen in green patches in KIL 82 (**f**). Plg: plagioclase, Opq: opaque minerals, Chp: chlorophaeite

### 3.3. P- and S-Wave Attenuation ( $Q_p$ , $Q_s$ )

Seismic wave attenuation is an important parameter which helps to understand the intrinsic rock properties as well as to interpret the field seismic data. It defines the loss of energy per cycle. A wave which has traveled some distance  $x$  will suffer a loss in its amplitude by a factor given by  $e^{-(\frac{f\pi}{QV})x}$ , where  $Q$  is attenuation,  $f$  the frequency, and  $V$  is the velocity. The attenuation can be quantified by  $1/Q$ , where  $Q$  is the quality factor. It can also be written as  $Q = 2\pi$  (total energy/energy lost during one cycle). Smaller  $Q$  results in faster damping thereby resulting into a greater deviation from the elastic case. In fact, when the seismic wave propagates through a geological medium, the elastic energy associated with the wave is gradually absorbed by the medium and eventually gets converted to heat. It is commonly known as anelastic attenuation. Seismic energy is also lost in scattering and because of these two mechanisms, total disappearance of the seismic wave may also happen. In seismic exploration experiments, seismic wave comprises both the compressional (P-wave) as well as shear (S-wave) waves. Attenuation of shear wave results from relaxation of the shear modulus ( $\mu$ ), while compressional wave attenuation results from the relaxation of both the shear ( $\mu$ ) as well as bulk ( $\kappa$ ) modulus.

In the case of Deccan basalts, the nature of compressional and shear wave attenuation has not yet been investigated systematically in laboratory. Hence, our present understanding of the mechanism responsible for the attenuation of seismic energy in basaltic rocks is limited. Therefore, an attempt has been made here to measure seismic wave attenuation properties of all the basalt cores using the ‘pulse broadening’ technique which involves the use of the pulsed ultrasonic double transducer experimental

arrangement as explained in Ramana and Rao (1974). This method enables to determine  $Q$  over a wide range of frequencies.

## 4. Geological Investigations

To help in the interpretation of acquired data on elastic and petrophysical properties, we carried out geological studies on the individual core samples, which provided some interesting observations.

### 4.1. Petrological Studies

The studied basalt cores are mostly fine to medium grained, rarely coarse-grained, and highly massive to vesicular in nature. Massive basalt core samples are heavy and greenish black to dark black in color with metallic luster. In comparison, vesicular samples, which are usually found at the top of the flows, are greyish brown to dark brown in color. Petrological and geochemical examination of these samples indicates that the studied basalt rocks are relatively Fe- and Mg-rich and silica-deficient in composition. These rocks basically contain plagioclase, pyroxene phenocrysts, and microphenocrysts and occasionally, altered olivine as major constituents and magnetite and secondary silicates as accessory minerals (Fig. 3a-f). Quite a few samples are extremely glassy in nature (Fig. 3a), while many of these contained abundant microlites and plagioclase laths (Fig. 3b, d-f). Some of the samples are filled with secondary minerals such as chlorophaeite (Fig. 3c, e), and other forms of silicates (Fig. 3d-f), formed mainly by alteration of pyroxene and plagioclase grains.

### 4.2. Geochemical Studies

In addition to the petrological studies, we carried out geochemical analysis of whole rock major oxides at the geochemical labs of the CSIR-NGRI, Hyderabad (India), by Phillips Magix PRO model PW 2440 wavelength dispersive X-ray fluorescence spectrometer coupled with automatic sample changer PW 2540 (Krishna and Govil 2007). This is a sequential instrument with single goniometer-based measuring

channel, covering the complete elemental range from F to U in the concentration levels of a few ppm to % level. The measured precision is between 1 and 2%.

$\text{SiO}_2$  content in the Ambenali Formation (first half of the borehole) varied in an extremely narrow range from 45.74 to 47.36 wt% with a mean of 46.64 wt%. However, in Poladpur Formation (bottom half of the sequence), its average concentration was almost 2.0 wt% higher at 48.51 wt% (range 47.06–50.35 wt%), thereby making it moderately more silicic than the Ambenali Formation basalts. These core samples are quite rich in  $\text{MgO}$  contents, which suggest that the original source rock was rich in pyroxene and olivine.  $\text{MgO}$  contents average around 8.11 wt% (range 7.49–9.42 wt%) for Ambenali Formation. In comparison, average  $\text{MgO}$  is little lower at 7.19 wt% (range 5.39–9.14 wt%) in Poladpur Formation, conforming to their higher  $\text{SiO}_2$  contents, as mentioned above. Apart from generally higher  $\text{MgO}$ , average  $\text{FeO}_T$  in Ambenali and Poladpur Formations are also high around 13.57 wt% (range 12.60–14.73 wt%) and 13.25 wt% (range 12.66–14.24 wt%), respectively, which is on the quite higher side of known tholeiitic basalts. These concentrations are well reflected in the petrophysical properties too.

## 5. Results

Results of all the elastic and petrophysical properties carried out on the Killari borehole samples along with estimated elastic modulus are collated in Table 1 and their Formation-wise averages, along with characteristic  $\text{SiO}_2$  and  $\text{FeO}_T$  contents, are included in Table 2. Their variation with depth is shown in Figs. 4, 5, 6 and 7.

### 5.1. Density and Porosity

The measured dry and saturated densities of 13 massive basalts from the Ambenali Formation varied in a narrow range from 2.81 to 3.00  $\text{g/cm}^3$  (mean 2.91  $\text{g/cm}^3$ ) and 2.83–3.01  $\text{g/cm}^3$  (mean 2.92  $\text{g/cm}^3$ ), respectively. Measured densities in both dry and saturated states are almost identical due to their intrinsically low porosity, which is on an average only about 1.2%. In contrast, however, the dry and

saturated density of the sole vesicular basalt sample from this formation is 2.24 and 2.40  $\text{g/cm}^3$ , respectively, which can be attributed to extremely high porosity of 16.6%.

Similarly, measured dry and saturated densities of the 14 massive basalt cores from the Poladpur Formation, varies from 2.80 to 2.94  $\text{g/cm}^3$  (mean 2.88  $\text{g/cm}^3$ ) and 2.80–2.95  $\text{g/cm}^3$  (mean 2.90  $\text{g/cm}^3$ ), respectively. Again, in this case, dry and saturated densities are almost equal due to extremely low porosity averaging 1.08%. We could measure seven samples of the vesicular basalt from this formation compared to the only one sample in case of the Ambenali Formation. The dry and saturated densities in these core samples varied from 2.28 to 2.71  $\text{g/cm}^3$  (mean 2.54  $\text{g/cm}^3$ ) and 2.43–2.79  $\text{g/cm}^3$  (mean 2.65  $\text{g/cm}^3$ ), respectively, which are higher than those recorded in the Ambenali Formation, primarily due to on an average relatively lower porosity of 10.6% in the Poladpur Formation. The variation of density and porosity with depth for both formations is shown in Fig. 4.

### 5.2. P- and S-Wave Velocity

Average P-wave velocity measured on dry and saturated samples of massive basalts from the Ambenali Formation are found to be 5.78 (range 4.91–6.48) and 5.93 (range 5.03–6.50) km/s, respectively, with corresponding  $V_s$  of 3.36 (range 3.02–3.68) and 3.45 (3.10–3.64) km/s. However, dry and saturated  $V_p$  in the vesicular basalt sample of this formation is very low at 3.76 and 3.67 km/s, respectively, with corresponding  $V_s$  of 2.57 and 2.47 km/s.

In comparison, average dry and saturated  $V_p$  in massive basalts of the Poladpur Formation, which is more silicic than Ambenali, are a little lower at 5.74 (range 4.76–6.23) and 5.85 (range 5.01–6.23) km/s, respectively, with corresponding  $V_s$  of 3.36 (range 2.88–3.59) and 3.42 (range 2.84–3.59) km/s. For vesicular basalts of this formation, averaged dry and saturated  $V_p$  are found to be 3.86 (range 3.14–4.63) and 4.05 (range 3.28–4.78) km/s, respectively, with correspondingly low  $V_s$  of 2.43 (range 1.99–2.88) and 2.35 (range 1.70–2.95) km/s. The variation in  $V_p$  and

Table 1

*Density, elastic moduli, P- and S-wave velocities and attenuation in Deccan basalt cores from KLR-I borehole, drilled in the epicentral region of the 1993 Killari earthquake region, Maharashtra (India)*

Sample	Depth (m)	$\rho$ (g/cm <sup>3</sup> )			$\phi$ (%)	$V_p$ (km/s)		$V_s$ (km/s)		Poisson's ratio		$E$ (GPa)		$Q_P$		$Q_S$		
		Dry	Sat	Part		Dry	Sat	Dry	Sat	Dry	Sat	Dry	Sat	Dry	Sat	Dry	Sat	
<b>Ambenali Formation</b>																		
KIL-66	20.4	M	2.89	2.91	2.96	2.4	5.63	5.84	3.14	3.44	0.28	0.24	72	84	1015	881	410	61
KIL-51	30.5	M	2.87	2.88	2.90	1.0	5.84	5.89	3.38	3.39	0.25	0.25	82	83	713	1304	148	124
KIL-67	39.6	M	2.91	2.92	2.94	1.0	5.90	5.94	3.41	3.42	0.25	0.25	84	85	630	1002	503	318
KIL-68	67.8	M	3.00	3.01	3.02	0.6	6.48	6.50	3.68	3.64	0.26	0.27	102	101	330	—	177	—
KIL-52	70.8	M	2.96	2.97	3.00	1.4	6.03	6.04	3.51	3.50	0.24	0.25	91	91	136	228	59	82
KIL-69	124.4	M	2.94	2.95	2.96	0.8	6.26	6.31	3.63	3.69	0.25	0.24	97	99	1196	—	108	48
KIL-70	134.6	M	2.95	2.96	2.96	0.3	6.27	6.32	3.64	3.66	0.25	0.25	98	99	33	102	31	53
KIL-71	145	M	2.90	2.90	2.92	0.7	5.81	6.14	3.12	3.43	0.30	0.27	73	87	177	286	110	170
KIL-72	148	M	2.91	2.91	2.92	0.5	5.96	6.14	3.53	3.64	0.23	0.23	89	95	61	696	38	66
KIL-55	152	M	2.91	2.93	2.97	1.8	5.99	6.07	3.49	3.44	0.24	0.26	88	87	—	—	158	—
KIL-73	164.4	M	2.81	2.83	2.87	1.8	4.91	5.03	3.02	3.10	0.20	0.20	61	65	42	44	38	49
KIL-74	168	M	2.87	2.88	2.91	1.5	4.99	5.49	3.08	3.29	0.19	0.22	65	76	51	60	49	43
KIL-56	171.5	M	2.86	2.87	2.90	1.6	5.11	5.34	3.07	3.15	0.22	0.23	66	70	95	91	67	42
KIL-53	96	V	2.24	2.40	2.68	16.6	3.76	3.67	2.57	2.47	0.06	0.09	31	30	7	6	6	6
<b>Poladpur Formation</b>																		
KIL-57	188.5	M	2.88	2.92	3.00	3.9	4.76	5.01	2.88	2.84	0.21	0.26	58	59	93	88	65	35
KIL-58	209.6	M	2.90	2.92	2.97	2.4	5.48	5.65	3.48	3.47	0.16	0.20	82	84	779	715	306	287
KIL-76	213.8	M	2.92	2.94	2.97	1.7	5.81	5.83	3.41	3.54	0.24	0.21	84	89	464	1960	61	49
KIL-77	216.3	M	2.94	2.95	2.97	1.3	5.70	5.69	3.35	3.48	0.24	0.20	81	86	116	136	57	78
KIL-85	258	M	2.90	2.90	2.91	0.3	6.18	6.23	3.51	3.51	0.26	0.27	90	91	—	—	949	506
KIL-62	265	M	2.80	2.80	2.81	0.6	5.71	5.72	3.33	3.34	0.24	0.24	77	78	64	61	59	55
KIL-82	269.7	M	2.80	2.82	2.84	1.4	5.48	5.60	3.37	3.34	0.20	0.22	76	77	23	33	24	47
KIL-83	271.85	M	2.87	2.88	2.89	0.6	5.86	5.89	3.31	3.36	0.27	0.26	79	82	53	44	21	26
KIL-63	279.6	M	2.92	2.93	2.94	0.4	6.15	6.15	3.48	3.48	0.26	0.26	90	90	339	498	129	130
KIL-84	287	M	2.91	2.91	2.92	0.3	6.23	6.23	3.59	3.59	0.25	0.25	94	94	—	—	47	83
KIL-87	317	M	2.82	2.84	2.87	0.5	5.17	6.03	3.10	3.43	0.22	0.26	66	86	56	65	40	41
KIL-65	327	M	2.89	2.90	2.91	0.6	5.97	6.03	3.45	3.49	0.25	0.25	86	86	225	437	75	47
KIL-88	327.1	M	2.92	2.93	2.94	0.6	5.88	5.93	3.47	3.49	0.23	0.24	87	88	288	270	50	79
KIL-89	332.45	M	2.91	2.91	2.92	0.5	5.93	5.95	3.36	3.46	0.26	0.24	83	87	2855	—	1132	—
KIL-75	196	V	2.65	2.74	2.92	9.4	3.64	3.91	2.19	2.04	0.22	0.31	31	29	13	30	11	12
KIL-59	220	V	2.68	2.75	2.89	7.3	4.00	4.36	2.62	2.46	0.12	0.27	41	41	12	17	15	13
KIL-78	226.6	V	2.71	2.78	2.91	6.8	4.39	4.64	2.56	2.70	0.24	0.24	44	49	27	46	33	49
KIL-79	231	V	2.73	2.79	2.91	6.3	4.63	4.78	2.88	2.95	0.18	0.19	54	56	42	44	29	49
KIL-60	241	V	2.28	2.43	2.68	15.0	3.14	3.41	2.17	2.19	0.04	0.15	22	25	9	11	5	6
KIL-61	243	V	2.47	2.60	2.83	12.7	3.91	3.97	2.60	2.44	0.11	0.20	37	35	10	19	10	5
KIL-80	250.2	V	2.30	2.46	2.75	16.6	3.30	3.28	1.99	1.70	0.22	0.32	22	17	7	6	7	5

M and V refer to massive and vesicular varieties of Deccan basalts and part refers to particle density

$V_s$ , together with their ratios with depth for both formations, is shown in Fig. 5.

### 5.3. Elastic Moduli

Elastic moduli are considered as one of the important rock properties to evaluate the stress-strain behavior of the rock. Young's modulus in massive basalt of both formations (Ambenali as well as

Poladpur) varies in the range 58–102 GPa in case of dry samples and is quite similar (59–101 GPa) in saturated samples. Higher values can be attributed to compactness and the resultant increase in grain contact area and grain contact stress in massive core samples, which are mafic in nature and have negligible porosity. Corresponding values of Young's modulus are found to be much lower in case of vesicular basalts; 22–54 GPa in dry samples, and

Table 2

*Average density, elastic moduli, P- and S-wave velocities and attenuation in Ambenali and Poladpur Deccan basalts formations, as encountered in KLR-1 borehole, drilled in the epicentral region of the 1993 Killari earthquake region, Maharashtra (India)*

Sample	$\rho$ (g/cm <sup>3</sup> )	$\phi$ (%)	$V_p$ (km/s)	$V_s$ (km/s)	FeOT (wt%)	SiO <sub>2</sub> (wt%)	$v$	$E$ (GPa)	$Q_p$	$Q_s$
<b>Ambenali Formation (dry samples)</b>										
Massive	2.91	1.20	5.78	3.36	13.56	46.64	0.24	82	373	146
(n)	13	13	13	13	13	13	13	13	12	13
Vesicular	2.24	16.55	3.76	2.57	13.71	46.62	0.06	31	7	6
(n)	1	1	1	1	1	1	1	1	1	1
Avg.	2.86	2.30	5.64	3.30	13.57	46.64	0.23	79	345	136
(n)	14	14	14	14	14	14	14	14	13	14
<b>Poladpur Formation (dry samples)</b>										
Massive	2.88	1.08	5.74	3.36	13.24	48.80	0.24	81	446	215
(n)	14	14	14	14	14	14	14	14	12	14
Vesicular	2.54	10.58	3.86	2.43	13.28	47.95	0.16	36	17	16
(n)	7	7	7	7	7	7	7	7	7	7
Avg.	2.77	4.25	5.11	3.05	13.25	48.51	0.21	66	288	149
(n)	21	21	21	21	21	21	21	21	19	21
Total avg.	2.81	3.47	5.32	3.15	13.38	47.77	0.22	71	311	144
(n)	35	35	35	35	35	35	35	35	32	35
Samples	$\rho$ (g/cm <sup>3</sup> )	$\phi$ (%V/V)	$V_p$ (km/s)	$V_s$ (km/s)	FeOT	SiO <sub>2</sub>	$v$	$E$ (GPa)	$Q_p$	$Q_s$
<b>Ambenali Formation (saturated samples)</b>										
Massive	2.92	1.20	5.93	3.45	13.56	46.64	0.24	86	469	96
(n)	13	13	13	13	13	13	13	13	10	11
Vesicular	2.40	16.55	3.67	2.47	13.71	46.62	0.09	30	6	6
(n)	1	1	1	1	1	1	1	1	1	1
Avg.	2.88	2.30	5.77	3.38	13.57	46.64	0.23	82	427	89
(n)	14	14	14	14	14	14	14	14	11	12
<b>Poladpur Formation (saturated samples)</b>										
Massive	2.90	1.08	5.85	3.42	13.24	48.80	0.24	84	392	112
(n)	14	14	14	14	14	14	14	14	11	13
Vesicular	2.65	10.58	4.05	2.36	13.28	47.95	0.24	36	25	20
(n)	7	7	7	7	7	7	7	7	7	7
Avg.	2.81	4.25	5.25	3.06	13.25	48.51	0.24	68	249	80
(n)	21	21	21	21	21	21	21	21	18	20
Total avg.	2.84	3.47	5.46	3.19	13.38	47.77	0.24	74	317	83
(n)	35	35	35	35	35	35	35	35	29	32

17–56 GPa in case of saturated samples, thereby closely reflecting the porous nature of these rocks. Similarly, Poisson's ratio in massive basalts varied from 0.16 to 0.30 in the dry state and 0.20–0.27 in saturated state. As in case of Young's modulus, corresponding values of Poisson's ratio in case of vesicular basalts are much lower; 0.04–0.24 in dry state and 0.09–0.31 in saturated state (Tables 1, 2). These two parameters vary significantly with depth from one formation to another (Fig. 6). Widespread chemical alterations, microcracks, and presence of vesicles, which are filled in by secondary minerals,

have substantially lowered the elastic moduli of the rock.

#### 5.4. Compressional and Shear Wave Attenuation

Data on measured attenuation and their ratios in Deccan basalts of both formations are given in Tables 1, 2 and 3, and their variation with depth is shown in Fig. 7. Table 1 reveals that the measured  $Q_p$  exhibits an extremely wide range of 33–1960 in saturated samples of massive basalts and 6–46 for vesicular basalts. In comparison, the saturated  $Q_s$  ranges from 26 to 506 in massive basalts and 5–49 in

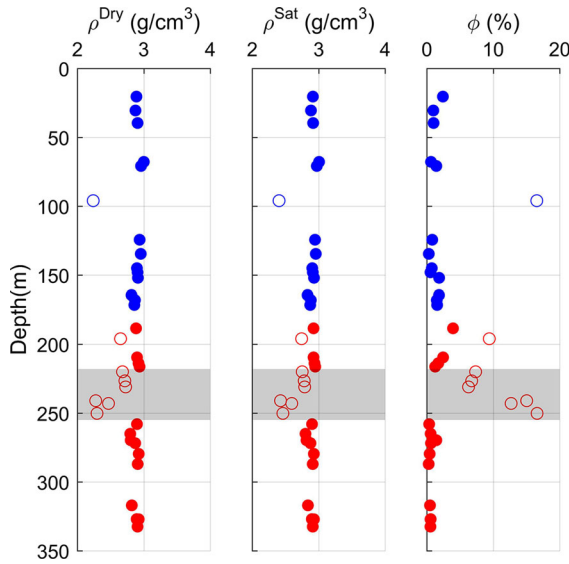


Figure 4

Variation of dry and saturated density and porosity with depth in Deccan basalt cores from Killari borehole. Solid and open blue circles refer, respectively, to massive and non-massive (vesicular) cores of Ambenali Formation while similar red circles to Poladpur Formation. Shaded area represents the location of the VIth flow from the top that belong to Poladpur Formation and appears totally vesicular

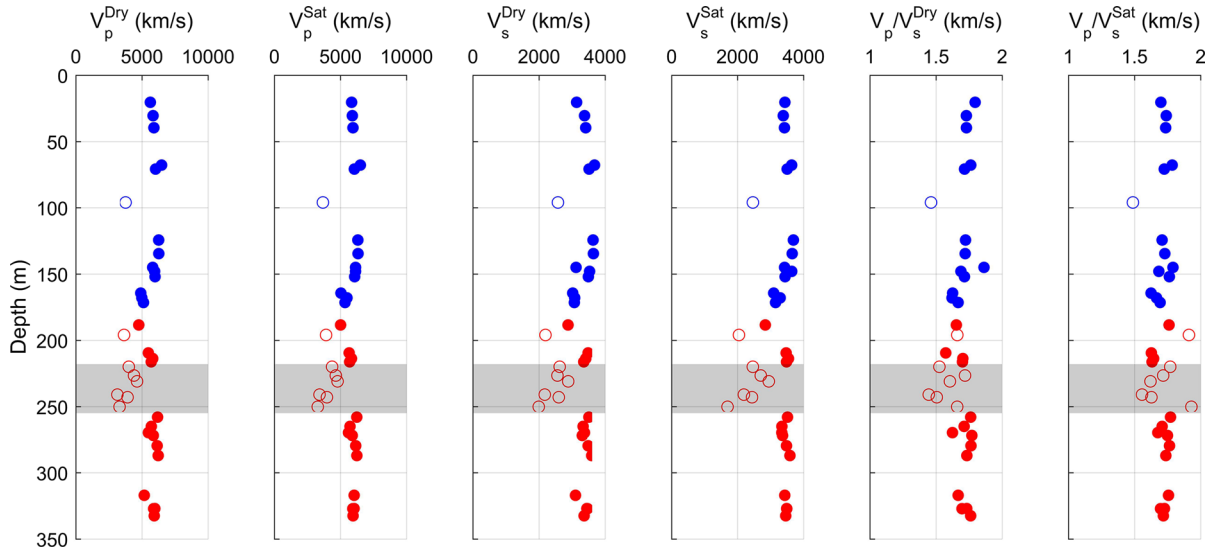


Figure 5

Variation of dry and saturated  $V_p$ ,  $V_s$  and  $V_p/V_s$  with depth in Deccan basalt cores from Killari borehole. Solid and open blue circles refer, respectively, to massive and non-massive cores of Ambenali Formation, while similar red circles to Poladpur Formation. Shaded area represents the location of the VIth flow from the top that belong to Poladpur Formation and appears totally vesicular

vesicular samples. Similarly, in case of dry samples,  $Q_p$  ranges from 23 to 2855 in massive and from 7 to 42 in vesicular ones. Correspondingly, dry  $Q_s$  ranges from 21 to 1132 in massive and 5–33 in vesicular basalts.

## 6. Discussion

The interpretation of geophysical data is highly dependent on laboratory-measured physical constraints like elastic and petrophysical properties of rocks, which can indirectly provide lithological information of underlying deeper horizons. For such studies, surface samples which are often weathered, are avoided. In this regard, Deccan basalt cores recovered from the Killari borehole provided a unique opportunity.

As can be seen from the depth-wise plots (Figs. 4, 5, 6, 7), as well as geochemical variations (Table 2) as discussed earlier, a distinction between Ambenali and Poladpur Formations is quite evident. It is not

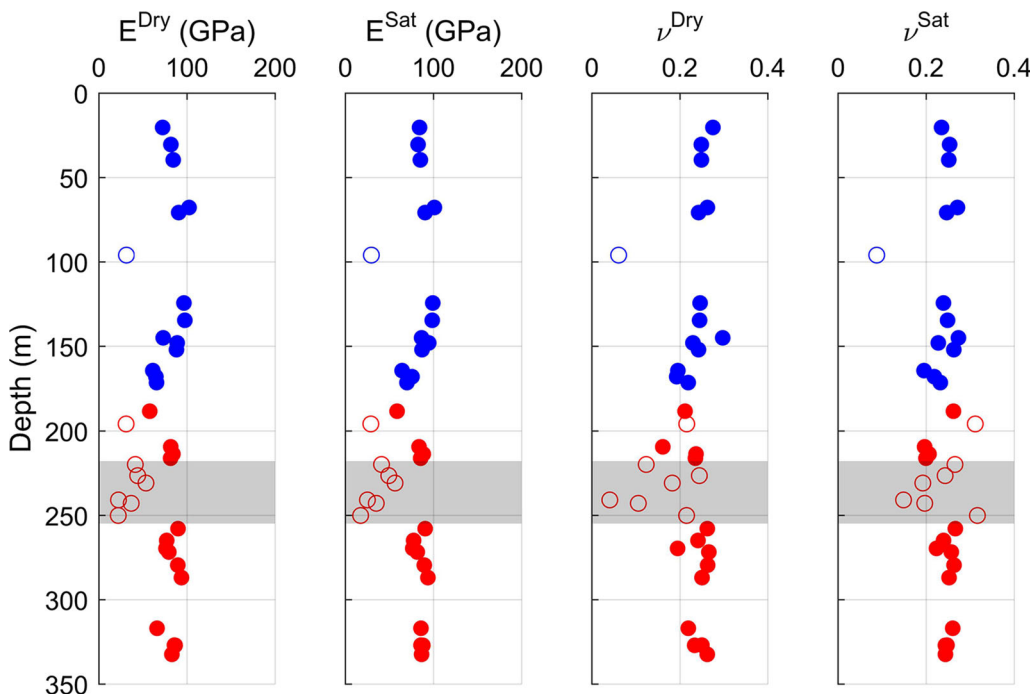


Figure 6

Variation of the Young modulus ( $E$ ) and the Poisson ratio's ( $\nu$ ) (dry as well as saturated) with depth in Deccan basalt cores from Killari borehole. Solid and open blue circles refer, respectively, to massive and non-massive cores of Ambenali Formation while similar red circles to Poladpur Formation. Shaded area represents the location of the VIth flow from the top that belong to Poladpur Formation and appears totally vesicular

surprising as the Ambenali Formation, which is one of the thickest units among the Deccan Trap flows and also the least contaminated by continental crust and the mantle lithosphere (Cox and Hawkesworth 1985; Beane et al. 1986; Mahoney 1988; Cox and Mitchell 1988; Sano et al. 2001), appears more mafic and has consistent petrophysical properties. This can be attributed to its relatively slow rate of crystallization.

In contrast, the Poladpur Formation is highly contaminated by crustal fractions, as revealed by their REE abundances. Usually, Ba elemental concentrations and Ba/Nb ratios are high in crustally contaminated rocks. In massive samples of Poladpur Formation, Ba concentrations and Ba/Nb ratios are quite high at 199.3 ppm and 16.3, respectively, compared to 79.5 ppm and 9.42 in Ambenali Formations. As a result of crustal contamination, Poladpur Formation has become silica-rich by almost

2 wt% than the Ambenali Formation, which conforms to petrophysical properties.

### 6.1. Mineral Composition

First and foremost thing we noticed about these basalt core samples is that both the formations as a whole, are rich in iron and magnesium oxide contents. They contain on an average higher amount of  $\text{FeO}_T$  (range 12.60–14.73 wt%; mean 13.38 wt%) as well as  $\text{MgO}$  (5.39–9.42 wt%; mean 7.56 wt%) than reported in earlier studies for similar formations, using mainly surface outcrop samples (Lightfoot et al. 1990; Sen 2001; Sen and Chandrasekharan 2011). Such higher values would suggest that these basalts are olivine-rich and primitive in nature. Usually, in the eastern part of the Deccan volcanic region,  $\text{MgO}$  content in Deccan basalts is reportedly much less compared to western Deccan Traps (Vijaya Kumar et al. 2010; Shrivastava et al. 2014). In fact,

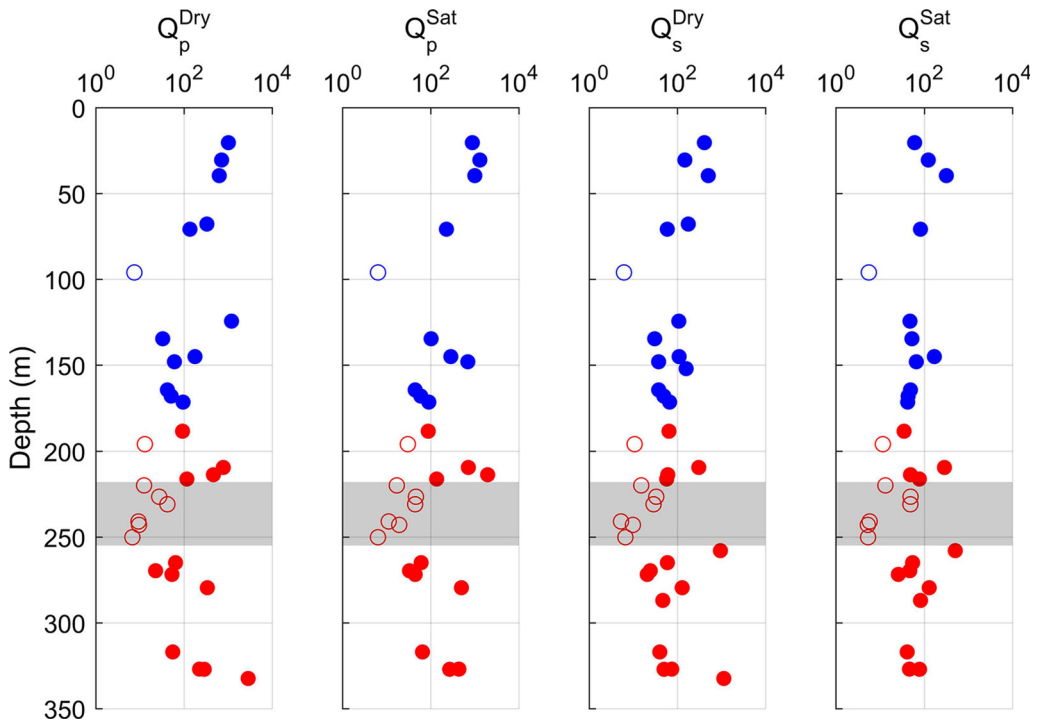


Figure 7

Variation of P- and S-wave attenuation ( $Q_p$ ,  $Q_s$ ) (in both dry and saturated states) with depth in Deccan basalts cores from Killari borehole. Solid and open blue circles refer, respectively, to massive and non-massive cores of Ambenali Formation while similar red circles to Poladpur Formation. Shaded area represents the location of the VIth flow from the top that belong to Poladpur Formation and appears totally vesicular

the erupted tholeiitic lavas are known to contain only about 5–7 wt% of MgO (Sen and Chandrasekharam 2011). Consequent to being Mg- and Fe-rich, the basalts of this region are also deficient in silica content (mean: SiO<sub>2</sub>: 47.8 wt%) (Table 2), compared to usual Deccan basalts samples (Chatterjee and Bhattacharji 2008; Lightfoot et al. 1990). This would also mean that these basalts are relatively more mafic than the Deccan basalts of other areas. Although differences in geochemical composition do exist between Ambenali and Poladpur Formations, such geochemical differences are hardly noticeable between massive and vesicular varieties of the same formation (Table 2).

## 6.2. Characteristic Elastic Properties

When we compare petrophysical properties of these two formations individually, it was observed that the massive cores of Ambenali Formation are

characterized by a little higher average saturated density (2.92 g/cm<sup>3</sup>) and  $V_p$  (5.93 km/s) compared to 2.90 g/cm<sup>3</sup> and 5.85 km/s, respectively, estimated for the massive cores of the Poladpur Formation (Table 2). As mentioned earlier, this can be ascribed partly to their non-contaminated nature and almost 2 wt% lesser SiO<sub>2</sub> content (46.64 wt%) as well as higher MgO contents (8.11 wt%) of the Ambenali Formation, which makes it more mafic than the Poladpur Formation that has lower MgO (6.8 wt%) as well as higher SiO<sub>2</sub> content (48.80 wt%). It is well known that  $V_p$  is negatively correlated with SiO<sub>2</sub> content (e.g., Rudnick and Fountain 1995), while MgO content has a positive impact on velocities (Table 2).

### 6.2.1 Unusual Petrophysical Nature of the VIth Flow and Possible Evolutionary Model

An interesting observation of this study has been the finding that the elastic and petrophysical properties of

Table 3

$V_p/V_s$  and  $Q_s/Q_p$  ratios in Deccan basalt cores as encountered in KLR-1 borehole, drilled in the epicentral region of the 1993 Killari earthquake region, Maharashtra (India)

S. no.	Sample name	Depth	Nature of basalt	$V_p/V_s$ dry	$V_p/V_s$ sat	$Q_s/Q_p$ dry	$Q_s/Q_p$ sat
1.	KIL-66	20.4	Massive	1.80	1.70	0.40	0.07
2.	KIL-51	30.5	Massive	1.73	1.74	0.21	0.10
3.	KIL-67	39.6	Massive	1.73	1.74	0.80	0.32
4.	KIL-52	70.8	Massive	1.72	1.72	0.43	0.36
5.	KIL-70	134.6	Massive	1.72	1.73	0.93	0.52
6.	KIL-71	145	Massive	1.86	1.79	0.62	0.59
7.	KIL-72	148	Massive	1.69	1.68	0.62	0.10
8.	KIL-74	168	Massive	1.62	1.67	0.96	0.73
9.	KIL-56	171.5	Massive	1.67	1.69	0.70	0.47
10.	KIL-57	188.45	Massive	1.65	1.76	0.70	0.40
11.	KIL-58	209.55	Massive	1.57	1.63	0.39	0.40
12.	KIL-76	213.8	Massive	1.70	1.64	0.13	0.02
13.	KIL-77	216.3	Massive	1.70	1.63	0.49	0.57
14.	KIL-62	265	Massive	1.71	1.71	0.92	0.90
15.	KIL-82	269.7	Massive	1.62	1.68	1.07	1.43
16.	KIL-83	271.85	Massive	1.77	1.75	0.39	0.58
17.	KIL-63	279.6	Massive	1.76	1.76	0.38	0.26
18.	KIL-87	317	Massive	1.67	1.76	0.72	0.63
19.	KIL-65	327	Massive	1.73	1.73	0.33	0.11
20.	KIL-88	327.1	Massive	1.70	1.70	0.17	0.29
21.	KIL-53	96	Vesicular	1.46	1.49	0.82	0.87
22.	KIL-75	196	Vesicular	1.66	1.91	0.83	0.38
23.	KIL-59	220	Vesicular	1.53	1.77	1.22	0.78
24.	KIL-78	226.6	Vesicular	1.72	1.72	1.21	1.06
25.	KIL-79	231	Vesicular	1.61	1.62	0.69	1.10
26.	KIL-60	241	Vesicular	1.45	1.56	0.57	0.52
27.	KIL-61	243	Vesicular	1.51	1.63	1.03	0.27
28.	KIL-80	250.2	Vesicular	1.66	1.93	0.98	0.84

the six Poladpur samples that come from the depth range between 220 and 250.2 m, are characterized by extremely low saturated mean density ( $2.64 \text{ g/cm}^3$ ), P- and S-wave velocities (4.07 and 2.41 km/s, respectively) and Young's modulus (37.2 GPa) (Figs. 4, 5, 6). Similarly, in those samples, saturated values of  $Q_p$  and  $Q_s$  are on an average also quite low at 23.8 and 21.2, respectively (Fig. 7), indicating a high level of attenuation. As per the studies of Gupta et al. (2003), this depth range (shaded in Figs. 4, 5, 6, 7) would correspond to the complete sequence of the VIth lava flow from the top (218.8–254.5 m). As per their studies, this flow contains about 7 m of massive basalts (between 226 and 233 m) and rest vesicular. However, the samples KIL-78 (226.6 m) and 79 (231 m) which belong to this depth range are found to be of vesicular in nature. A petrographic study carried out on a thin section of one of these (KIL-79), does

confirm that it is highly altered and contains a high amount of secondary silicate minerals as well as chlorophaeite (Fig. 3e). Entire VIth flow thus appears totally vesicular, which is highly unusual considering that all other flows have vesicular/amygdaloidal basalts at the top and massive basalts at the bottom. The considerable lowering in petrophysical attributes of this flow appears closely related to the enhanced porosity, which is around 10.8%. Therefore, it may be possible to differentiate the nature of flows based on petrophysical characteristics.

Keeping in mind the petrophysical and geochemical nature of this flow, it appears that the magma was volatile-rich, which got deposited at the surface in quick succession. It is not surprising since Deccan Traps are known to be associated with highest rates of eruption (Walker 1993) and if we take the figure suggested by Sen et al. (2006), the actual

duration of Deccan eruption was only 30,000 years, then its eruption rate comes to as high as 3.5 million kg of basalt per second. Considering the above-mentioned factors, we believe that the rate of eruption of this flow could have been still higher with rapid cooling and consequently, volatiles could not fully escape. Besides, this flow subsequently underwent hydrothermal alteration and recrystallization. Hydrothermal alterations do influence the elastic parameters.

Furthermore, since this flow is also crustally contaminated, it should have been erupted through secondary magma chambers at upper crustal depths. This conjecture is amply supported by Fig. 8 (Pandey 2008), from which two inferences can be drawn. Firstly, 4- to 5-km-thick high-velocity primitive Deccan magma (peridotitic/eclogitic; Sen and Chandrasekharam 2011) has underplated the Moho, and secondly, from 5 km onwards to about 20 km depth from the surface, crustally contaminated Deccan magma is still present, which did not get erupted.

### 6.3. Relationship Among, Elastic and Petrophysical Parameters

Elastic and petrophysical characteristics of the rocks are known to be greatly affected by pore fluid pressure and frequency range used for the

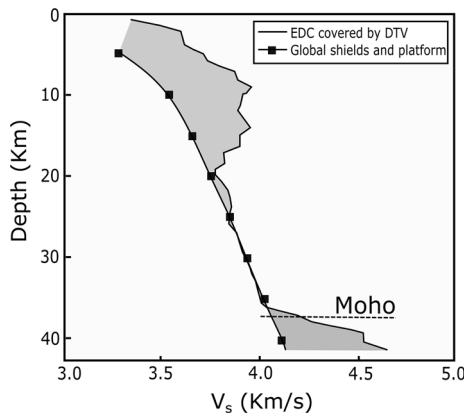


Figure 8

S-wave velocity distribution beneath Deccan Trap volcanic (DTV) covered block of the Eastern Dharwar Craton (EDC). For comparison, average S-wave velocity distribution (converted from P-wave velocity; Christensen and Mooney 1995) beneath global shields and platforms is also included. Moho depth is shown by dashed line (after Pandey 2008)

observation, besides, mineral composition, their geological evolution and subsequent alteration. (Kern et al. 1993, 2009; Tripathi et al. 2012b; Pandey et al. 2016). Therefore, it is often not possible to directly relate density to ultrasonic wave velocities or the intrinsic attenuation. As the petrophysical properties bear the imprints of paleo-geological processes, their inter-relationship can reveal whether the studied rock has undergone any major alteration subsequently after their initial emplacement or not.

#### 6.3.1 Density and Porosity

Figure 9 reveals almost a linear relationship between dry as well as saturated densities and porosity, across the entire basalt flow sequence drilled at Killari, indicating that the density of the solid phase may be directly related to the measured density. Since basalts are mainly composed of plagioclase and pyroxene minerals, these are highly susceptible to alteration due to the mobilization of volatiles and hydrous fluids through the thin cracks (or fractures). This is especially true for the plagioclase mineral-rich rocks like basalt. In this rock, it constitutes almost 30–40% of the rock matrix and has two sets of cleavage (or weak zones) that cause weak binding. Chemically altered products like secondary minerals, which are highly hydrous, like chlorophaeite, clays, sericite, chlorite, epidote, etc., effectively seal such cracks. Their presence (Fig. 3c–f) invariably lowers the particle (or grain) density as well as moduli of the rock, thus correlating with increasing porosity (Christensen et al. 1980; Carlson and Herrick 1990). In view of this, we calculated particle density of all the samples (mass per unit volume of the solid portion) using the relation: Particle density = dry density/(1 + dry density – wet density), where water is taken as having unit density. Then we made a cross plot between particle density and porosity, as shown in Fig. 10 which further corroborates that particle density of solid phase consistently decreases linearly with porosity.

#### 6.3.2 $V_p$ , $V_s$ and Porosity

Figure 9 also shows a possible relationship between  $V_p$ ,  $V_s$  and porosity. Like density, both these

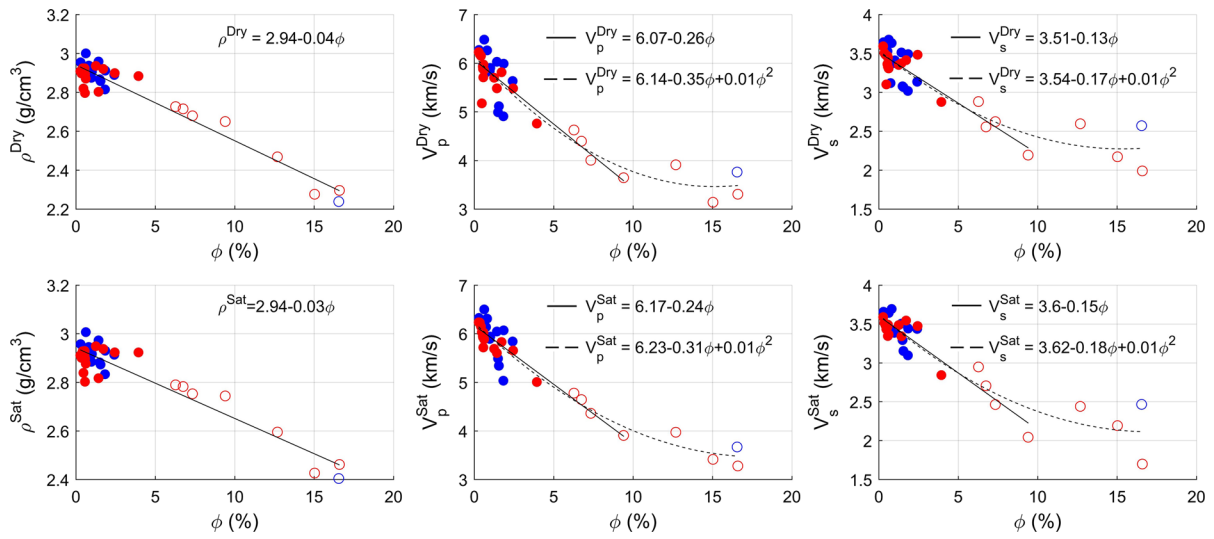


Figure 9

Plots of density ( $\rho$ ), P-wave velocity ( $V_p$ ) and S-wave velocity ( $V_s$ ), versus porosity ( $\phi$ ) in both dry as well as saturated states for Deccan basalt cores from Killari borehole. Solid and open blue circles refer, respectively, to massive and non-massive cores of Ambenali Formation while similar red circles to Poladpur Formation. Linear regression fit is represented by solid line, while polynomial regression fit by dashed line

parameters decrease with increase in porosity, but a reasonable linear relationship is seen till the porosity does not exceed 10%. However, a second-order polynomial regression model can be fitted through the entire data, as shown by dashed line, which reveals that velocities decrease more rapidly with

porosity, till the aforesaid limit is reached, but once it is exceeded, velocity drop is more gradual. Further, the plots between both P-wave and S-wave velocities and porosity, reveal a similar pattern, which would indicate that beyond 10% porosity, the presence of secondary minerals in the matrix of the sample dominates the velocities, rather than saturation. In such case it is not surprising to see a similar polynomial fit between velocities and density (Fig. 11) and almost one to one relationship between  $V_p$  and  $V_s$  (Fig. 12).

Based on the above inferences, we believe that the porosity is a major microstructural controlling parameter over both density and velocity. However, since the velocities of saturated and dry samples exhibit almost similar variation with the porosity (Fig. 9), the modulus of the rock matrix too might be contributing towards velocity changes, especially once porosity increases beyond 10%. The addition of the alteration products to the rock matrix lowers the grain density and apparent grain bulk and shears moduli of the rock and thus also lowers the P-wave and S-wave velocities (Cerney and Carlson 1999).

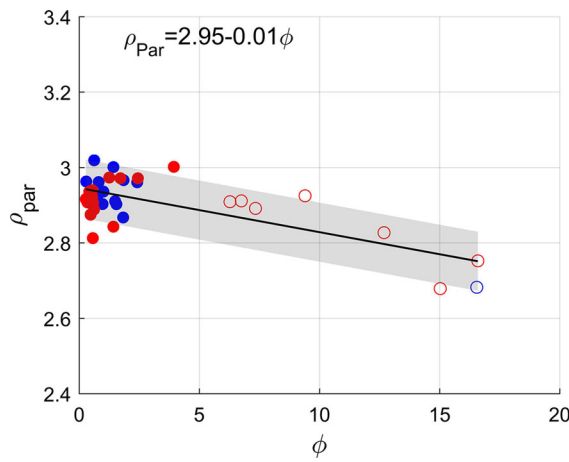


Figure 10

Cross-plot between particle density ( $\rho_{\text{par}}$ ) and porosity ( $\phi$ ) for Deccan basalt cores from Killari borehole. Solid and open blue circles refer, respectively, to massive and non-massive cores of Ambenali Formation while similar red circles to Poladpur Formation. The shaded area around the linear fit line shows one standard deviation bounds

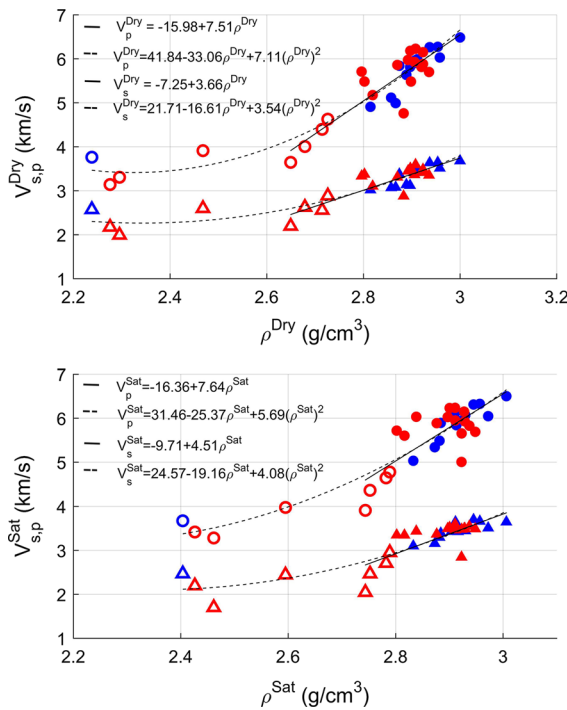


Figure 11

Variation of  $V_p$  (circles) and  $V_s$  (triangles) versus density (for both dry and saturated states) for Deccan basalt cores from Killari borehole. Blue solid circle/triangle: massive Ambenalli; red solid circle/triangle: massive Poladpur; blue open circle/triangle: vesicular Ambenalli; red open circle/triangle: vesicular Poladpur. Linear regression fit is represented by solid line, while polynomial regression fit by dashed line

### 6.3.3 Ultrasonic Wave Attenuation and Petrophysical Properties

In general, high-porosity rocks exhibit high attenuation and thus, as expected, seismic attenuation is found to be quite high ( $Q_p = 6\text{--}46$ ,  $Q_s = 5\text{--}49$ ) in highly porous saturated vesicular Deccan basalts. But surprisingly, some of the massive basalt core samples too exhibited high attenuation (Table 1). Petrological studies show that these non-porous massive basalts are often glassy in nature (Fig. 3a). Many of these are highly altered and contain secondary minerals like chlorophaeite (Fig. 3c, e) and other forms of secondary silicates which are hydrous in nature (Fig. 3d-f). Some of these samples have also shown conchoidal fractures. We therefore believe that the heterogeneities (like alteration, secondary mineral inclusion, glassy as well as its devitrified components like chlorophaeite) as mentioned earlier, are responsible for seismic energy loss in basalts samples and that's why attenuation of compressional and shear wave is high even in some of the massive basalt core samples like KIL-73, 74, 82 and 87.

As mentioned earlier, very little attenuation data are available on basalts. Interestingly, however, in comparison to Deccan basalts, oceanic basalts from Pacific (ODP holes 594B and 896A) and Atlantic (holes 395A) oceans, have shown  $Q_p$  variation from 5 to 35, and  $Q_s$  from 10 to 100 (Goldberg and Sun 1997).  $Q_p$  and  $Q_s$  values for oceanic basalt thus tend to conform to values for vesicular Deccan basalt, but

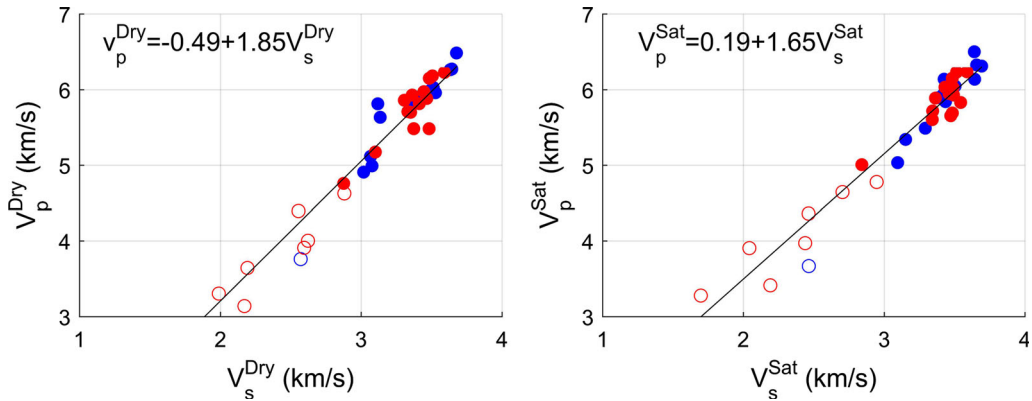


Figure 12

A plot between  $V_p$  and  $V_s$  (for both dry and saturated states) in Deccan basalt samples from Killari borehole. Solid and open blue circles refer, respectively, to massive and non-massive cores of Ambenali Formation, while similar red circles to Poladpur Formation

not to values for massive basalt. This would mean that the oceanic basalts are not massive, due to their possible formation by rapid cooling. Not surprisingly, therefore, Lewis and Jung (1989), Wepfer and Christensen (1990, 1991) and White and Clowes (1994) indicated a close correlation between low velocity, high crack/fracture porosity, a high degree of alteration and low  $Q_p$  (i.e., high attenuation). Since, ultrasonic wave characteristics are also known to be dependent on the physical properties of the rock (Wepfer and Christensen 1991), we plotted compressional and shear wave attenuation ( $Q_p$  and  $Q_s$ ) variation with depth (Fig. 7), as well as against measured porosity, density, and velocity (Figs. 13, 14, 15). Lewis and Jung (1989) mentioned that such type of dependence, as observed for ultrasonic frequencies, may exist at seismic frequencies also. This would mean that we can roughly estimate the expected value of attenuation of compressional and shear waves, based on available density and porosity values while carrying out seismic modeling experiments.

As can be seen from Figs. 13, 14 and 15, seismic wave attenuation increases with increase in porosity but decreases with increase in density, as well as  $V_p$  and  $V_s$ . In contrast to the finding of Tompkins and Christensen (2001), we observe a nearly linear trend in P-wave and S-wave attenuation data. However, scatter is quite high in case of the cores having high-density ( $> 2.9 \text{ g/cc}$ ) and low-porosity ( $< 2\%$ ) rocks. Basalts core samples with density  $< 2.8 \text{ g/cm}^3$  are highly attenuating. However, the attenuation in high-density and low-porosity massive basalt cores is not very sensitive to variation in density and porosity (Table 1), but possibly reflects dependence on the mineral composition of the rock matrix, as mentioned earlier. As shown in Fig. 15, the P- and S-wave quality factor increases linearly with increase in velocity, but after a cut off velocity of 5500 m/s (P-wave) and 3300 m/s (S-wave), the relation becomes non-linear. This would again mean that composition and intrinsic nature of basalt is playing a major role in seismic energy loss and this should be investigated in detail to quantify internal friction attenuation

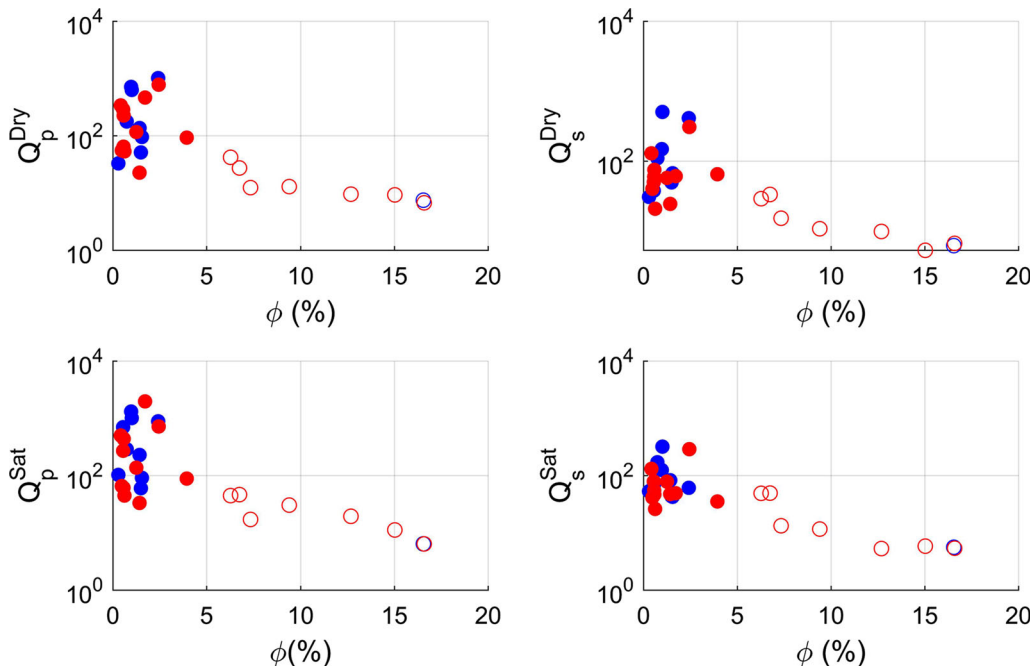


Figure 13

Relationship between measured  $Q_p$ ,  $Q_s$ , and porosity in Deccan basalt cores from Killari borehole. Solid and open blue circles refer, respectively, to massive and non-massive cores of Ambenali Formation, while solid and open red circles refer, respectively, to massive and non-massive cores of Poladpur Formation

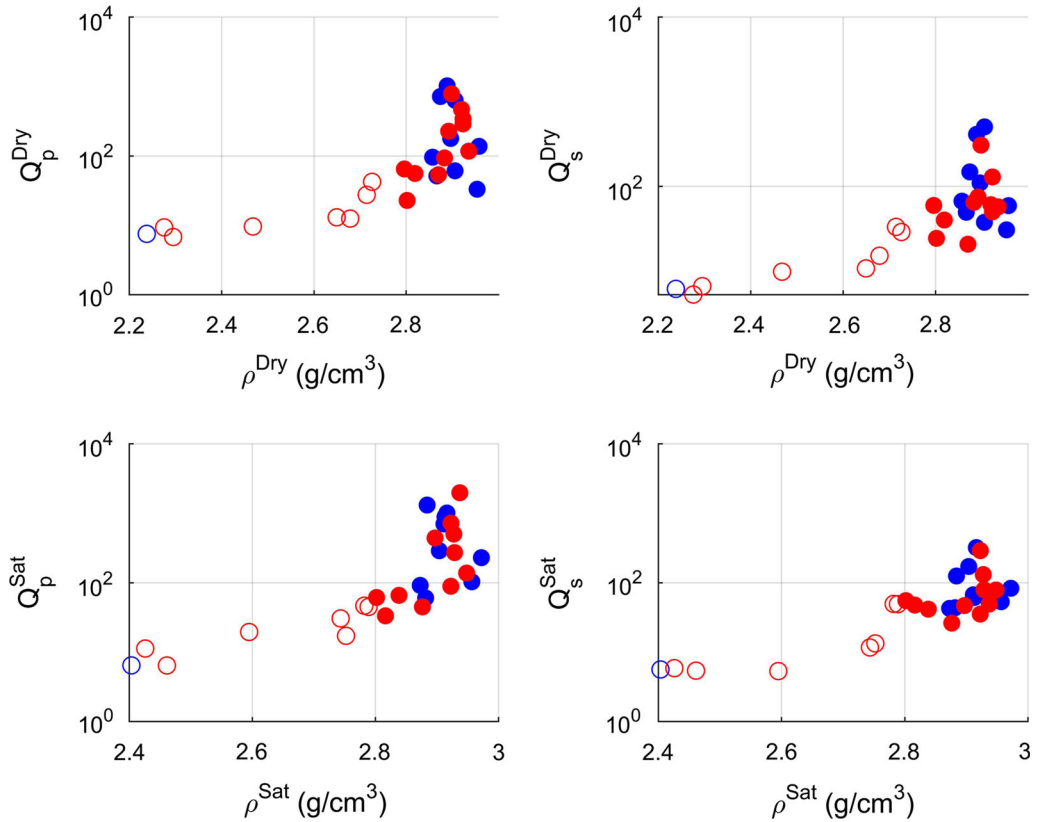


Figure 14

Variation in measured  $Q_p$ , and  $Q_s$  with density ( $\rho$ ) in Deccan basalt cores from Killari borehole. Solid and open blue circles refer, respectively, to massive and non-massive cores of Ambenali Formation, while solid and open red circles refer, respectively, to massive and non-massive cores of Poladpur Formation

mechanism as described by Weiner et al. (1987) for tholeiitic basalts. To further study the effect of pore fluids, we computed  $Q_s/Q_p$  and  $V_p/V_s$  values for the basalt core samples (Table 3) and plotted them in Fig. 16. The figure reveals that a very feeble inverse relationship exists between  $Q_s/Q_p$  and  $V_s/V_p$  in case of dry samples, but no such relationship is found in saturated core samples.

#### 6.4. Mechanism of Seismic Wave Energy Attenuation

Winkler and Nur (1982) and Murphy (1982) mentioned that for fully saturated core samples,  $Q_s/Q_p$  should be  $< 1$ , which is observed for most of our samples, except five samples. Out of these five samples, four samples (KIL-59, KIL-61, KIL-78, and KIL-79) represent very porous vesicular basalt. It is a known fact that attenuation measurement in highly porous vesicular basalt is relatively complicated

(Vedanti et al. 2015). The other such sample is KIL-82, which exhibited anomalous  $Q_s/Q_p$  saturated value of 1.43. Though this sample is massive, it is also highly altered and contain moderately abundant glass, apart from a large amount of infilled secondary hydrous minerals, as shown by green patches in Fig. 3f.

The value of  $Q_s/Q_p < 1$  would mean that for fully saturated rock, shear attenuation is higher than the compressional attenuation, because of “squirt flow” mechanism (Tompkins and Christensen 2001). Ideally,  $Q_s = Q_p$  for dry rock measurements or sometimes  $Q_s$  is slightly lower than  $Q_p$  in dry rocks, but in the present study, we observed  $Q_s/Q_p < 1$  for most of the oven-dried low-porosity samples, except the anomalous sample KIL-82, as discussed above. The mechanism for high attenuation of the shear wave as compared to P-wave attenuation in this sample, in the absence of pore fluid, could be a highly altered rock matrix. Since

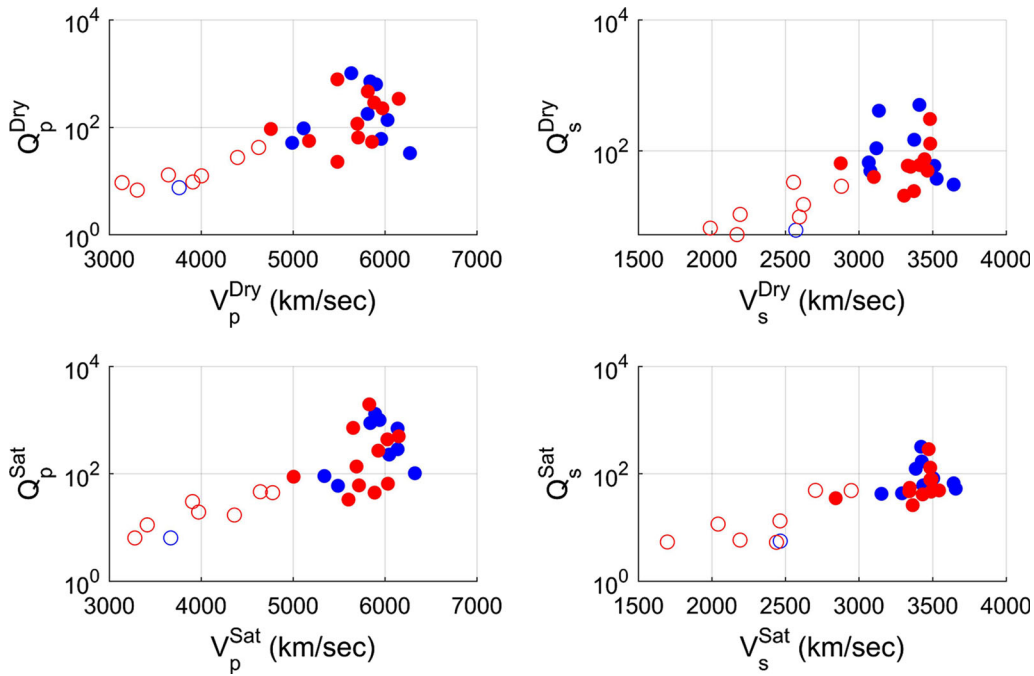


Figure 15

Variation in measured  $Q_p$  and  $Q_s$  with velocities in Deccan basalt cores from Killari borehole. Solid and open blue circles refer, respectively, to massive and non-massive cores of Ambenali Formation, while solid and open red circles refer, respectively, to massive and non-massive cores of Poladpur Formation

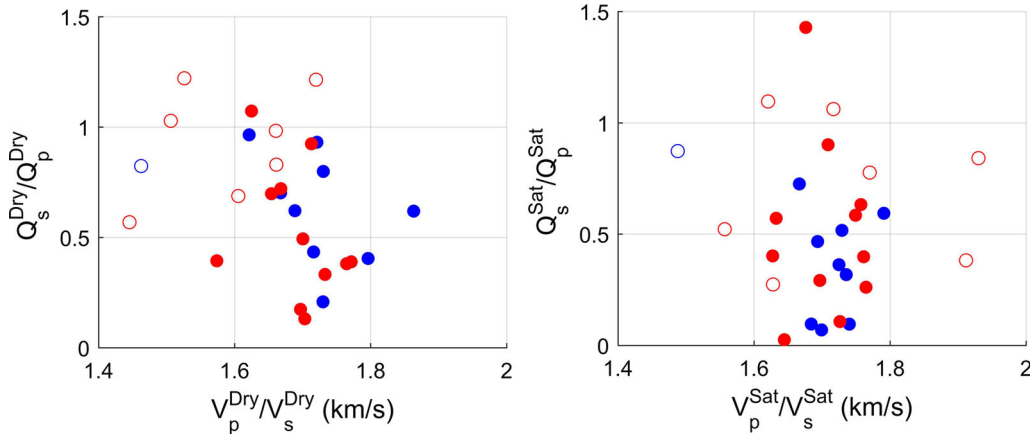


Figure 16

Plot of  $Q_s/Q_p$  versus  $V_p/V_s$  for the core samples of Deccan basalt from Killari borehole. Solid and open blue circles refer, respectively, to massive and non-massive cores of Ambenali Formation, while solid and open red circles refer, respectively, to massive and non-massive cores of Poladpur Formation

we observe a lower value of shear wave quality factor even in low-porosity dry samples, we argue that composition of the basalt is a major contributing factor towards attenuation. Relaxation of shear stresses in

weaker grain boundary material (altered minerals), and stress concentration at grain corners may cause the very low value of  $Q_s$  as compared to  $Q_p$ , which can be investigated in further studies.

Further, Tompkins and Christensen (2001) mentioned that a combination of  $Q_s/Q_p$  and  $V_p/V_s$  can characterize the saturation state of the rock but as we can see from Fig. 16, it is hard to distinguish between dry and saturated samples. A quick glance at  $V_p/V_s$  values obtained for saturated cores (with  $Q_s/Q_p < 1$ ) indicates that our results for Deccan basalt are different from the results published by Winkler and Nur (1982) for the saturation state of sandstones, which is altogether a different rock of sedimentary origin dominated by silica content, unlike basalts, which are mafic.

It is worth mentioning here that seismic attenuation observed in any rock is given as a sum of intrinsic anelastic attenuation and attenuation due to scattering. However, Wepfer (1989), Goldberg and Yin (1994) argued that at ultrasonic frequencies, only intrinsic attenuation dominates the attenuation of seismic energy. The major factor responsible for intrinsic anelastic attenuation is an internal frictional energy loss, which is either related to the dry rock frame or viscous fluid flow or both and it is difficult to quantify these parameters. Tisato and Quintal (2014) demonstrated that rock frame and fluid-related attenuation mechanisms are mutually independent. The frame-related attenuation is affected by strain, but does not vary with frequency; hence it might be more useful in seismic modeling experiments. However, the fluid-induced attenuation is frequency dependent. It has been shown in the literature that the rock properties including attenuation of seismic energy, measured in the laboratory may scale upwards with the wavelength. Thus, detailed investigations are further needed to uncover the physics of seismic wave attenuation.

#### *6.5. Representative Density and P- and S-Wave Velocity for Deccan Basalts*

A problem is often faced while assigning density and velocity values during the modeling of the geophysical data acquired over the Deccan volcanic terrain, as very little is known about the variation of petrophysical properties with depth. In view of this, we made an attempt to estimate average density and velocities of the volcanic sequence penetrated by Killari borehole, which may be representative for the

Deccan Volcanic Province, simply because this region consists of Ambenali and Poladpur Formations (Jay and Widdowson 2008) and their cumulative thickness in Western Ghats region (where the thickness of Deccan basalts are maximum), is approximately 800–900 m (Sano et al. 2001).

For this purpose, we use the density log provided by Gupta et al. (2003) to delineate the thicknesses of massive and vesicular strata in each formation and then assign the measured average values for them, as obtained from the present study (Tables 1, 2). This results in a weighted mean saturated density of 2.74 g/cm<sup>3</sup> for the entire Deccan volcanic sequence. Corresponding weighted mean values of saturated P-wave and S-wave velocities for this sequence are found to be 5.00 and 3.00 km/s, respectively.

#### *6.6. High-Density and Low P-Wave Velocity in Massive Basalts: Possible Cause*

As discussed above, ambiguities in crustal seismic studies still persist because of the dependence of seismic velocities on numerous factors, such as in situ conditions, mineralogy, density, and porosity apart from micro-fracture and chemical alteration. For example, deep seismic sounding studies carried out over Deccan volcanic terrain, consistently revealed extremely low  $V_p$  (4.50–5.25 km/s) in Deccan basalts, both in offshore as well as the onshore environment (Dixit et al. 2010; Murty et al. 2010, 2011, etc.). We too got similar values. The averaged  $V_p$  value measured in this study for the Deccan volcanic sequence at Killari is only 5.00 km/s, with a weighted density of 2.74 g/cm<sup>3</sup>. In normal crust, against such a density, P-wave velocity would be around 6.0–6.1 km/s (Christensen and Mooney 1995), instead of 5.00 km/s, which is almost 16% lower than the expected value. Even in the case of massive basalt cores, which have a high density of about 2.90 g/cm<sup>3</sup> (Table 2), measured  $V_p$  is only 5.85–5.93 km/s. P-wave velocities against such a high-density value should have been around 6.60 km/s (Christensen and Mooney 1995).

The existence of such low velocities in basaltic rocks against their average high density has not been understood so far. Normally, the drop in in situ

velocities are often ascribed to fluids, chemical alterations, serpentinization, microcracking, high mean atomic weight, presence of glass contents and vesicles, apart from low density and high porosity (Birch 1961a, b; Christensen 1968; Moose and Zoback 1983; Tompkins and Christensen 2001; Kern et al. 2009; Ullemeyer et al. 2011; Sun et al. 2012; Tripathi et al. 2012b; Pandey et al. 2016). However, we believe that in the present case, the lowering of velocities, especially in massive basalt cores in particular which have negligible porosity, can be primarily attributed to the presence of fine-grained glassy material (Fig. 3a), high iron (magnetite) contents (Fig. 3b–f), but more importantly to the inclusion of various forms of secondary minerals as a replacement altered product from the pyroxenes and plagioclase, which dominate the lithology (seen as green colored minerals in Fig. 3d–f). For example, chlorophaeite is one such secondary mineral, as seen in orange-brown color in Fig. 3c, e which occurs commonly in the Deccan basalts, along with other secondary minerals that may contain 10–20% of water content (Parthasarathy et al. 2003; Parthasarathy 2006). Chlorophaeite is a devitrified form of glass, often formed due to hydration of the original glass formed during rapid cooling of the magma or hydrothermal alteration of ferromagnesium minerals.

Further, most of the samples containing glassy basalts have shown the higher order of the seismic attenuation. Presence of iron in rocks increases the density but affects  $V_p$  adversely. Its enrichment can lead to significant velocity drop even in high-density rocks, due to increase in mean atomic weight of the rock sample (Birch 1961a, b; Christensen 1968; Pandey et al. 2016). As per Christensen (1968), for a constant density, higher mean atomic weight will result in lower velocity. Almost all the samples studied here are in general characterized by quite high  $\text{FeO}_T$  content (Table 2), in fact, the value of  $\text{FeO}_T$  content in these basalts (around 13.4 wt%) is more than the  $\text{FeO}_T$  content in the upper mantle. Even in case of the non-massive basalts, the velocity drop could be due to iron enrichment apart from the increased percentage of secondary minerals and porosity.

## 6.7. Conclusions

Our study provides a comprehensive new data set on the petrophysical and elastic properties of the 338-m-thick Ambenali and Poladpur Formations, pierced by the KLR-1 scientific borehole drilled in the 1993 Killari earthquake region of Maharashtra. Based on this study, some interesting inferences can be drawn about the geological, petrophysical and seismic attenuating characteristics of Deccan basalts, which are hitherto not too well known.

1. The saturated massive basalt cores of the Deccan volcanic sequence are characterized by a mean density of  $2.91 \text{ g/cm}^3$  and mean P- and S-wave velocities of 5.89 and 3.43 km/s, respectively. In comparison, vesicular basalts show a much lower density of  $2.62 \text{ g/cm}^3$  as well as P- and S-wave velocities of 4.00 and 2.37 km/s, respectively.
2. An almost inverse linear relationship exists between dry and saturated densities and porosity across the entire sequence, indicating that the density of the solid phase may be directly related to the measured density. Like density,  $V_p$  and  $V_s$  too decrease with increase in porosity. However, a reasonable linear relationship is seen only till the porosity reaches 10%, beyond which the velocity drop is more gradual indicating the dominance of the secondary minerals in the matrix over velocities, rather than saturation.
3. Porosity is a major microstructural controlling parameter over both density and velocity. However, since the P- and S-wave velocities of saturated and dry samples exhibit almost similar variation with the porosity, the modulus of the rock matrix too might be contributing to velocity changes, especially when porosity exceeds 10% threshold.
4. Compared to density and velocities, quality factors  $Q_p$  and  $Q_s$  in saturated massive basalts, vary enormously from 33 to 1960 and 26 to 506, respectively. However, the variation is somewhat lower ( $Q_p$  6–46;  $Q_s$  5–49) in saturated vesicular basalts, indicating the extremely high order of seismic attenuation. Such low values conform to  $Q_p$  and  $Q_s$  values of oceanic basalts, which too may be vesicular. High order of attenuation is also seen in some massive basalt cores. Such samples

are either glassy in nature or contain chlorophaeite and other secondary mineral products. Further, the seismic wave attenuation increases with increase in porosity, but decreases with increase in density, as well as  $V_p$  and  $V_s$ .

5. Since we observe a lower value of shear wave quality factor even in low-porosity dry samples, we argue that composition of the basalt is also a major contributing factor towards attenuation.
6. The Deccan basalt sequence at Killari is iron/magnesium-rich and relatively silica-deficient (average wt%, FeO<sub>T</sub>: 13.4; MgO: 7.56; SiO<sub>2</sub>: 47.8), possibly derived from the primitive mantle. As a whole, it is characterized by a weighted mean density of 2.74 g/cm<sup>3</sup>. Corresponding  $V_p$  and  $V_s$  values are quite low at 5.00 and 3.00 km/s, respectively, which is almost 15% lower than expected for such a density. The velocity drop can largely be attributed to the presence of glassy material, high iron contents, and large-scale inclusion of secondary minerals formed during hydrothermal alteration, that modified the original rock matrix and led to the reduction in particle density and consequently, higher porosity. Hydrous secondary minerals are known to contain as high as 10–20% of water content.
7. Petrophysical and petrologic studies indicate that the entire VIth lava flow from the top (218.8–254.5 m) is vesicular in nature, unlike other flows which have around 50% massive component. Magma derived for this flow may be rich in volatiles, which was deposited at the surface in quick succession and underwent rapid cooling and hydrothermal alteration. Further, it might have erupted through secondary magma chambers at upper crustal depths, as indicated by key geochemical parameters.

#### Acknowledgements

We thank Drs. K.J.P. Lakshmi, Kesav Krishna and M. Satyanarayanan for petrophysical and geochemical analysis and Drs. D. V. Subbarao and Dinesh Pandit for petrological examination of the thin sections and many useful discussions. We are also thankful to Prof.

Mrinal K. Sen, Ex-Director, CSIR-National Geophysical Research Institute, Hyderabad, for making available the samples for the analysis. This study has been supported by CSIR project SHORE PSC 0205. Dr. O.P. Pandey is thankful to CSIR for emeritus scientist position at CSIR-NGRI. One of the authors (AM) acknowledges UGC for providing Senior Research Fellowship. Further, highly constructive suggestions made by the anonymous reviewer and Prof. Y. Gueguen, Editor, Pure and Applied Geophysics, have been very helpful in improving the manuscript. Permission accorded by the Director CSIR-NGRI to publish this work, is also gratefully acknowledged.

#### REFERENCES

- Beane, J. E., Turner, C. A., Hooper, P. R., Subbarao, K. V., & Walsh, J. N. (1986). Stratigraphy, composition and form of the Deccan Basalts, Western Ghats, India. *Bulletin Volcanology*, 48, 61–83.
- Birch, F. (1960). The velocity of compressional waves in rocks to 10 Kilobars, part 1. *Journal of Geophysical Research*, 65, 1083–1102.
- Birch, F. (1961a). Composition of the earth's mantle. *Geophysical Journal of Royal Astronomical Society*, 4, 295–311.
- Birch, F. (1961b). The velocity of compressional waves in rocks to 10 kilobars, part 2. *Journal of Geophysical Research*, 66, 2199–2224.
- Brown, E. T. (1981). *Rock characterization testing and monitoring: ISRM suggested methods*. Oxford, New York: International Society of Rock Mechanics.
- Carlson, R. L., & Herrick, C. N. (1990). Densities and porosities in the oceanic crust and their variation with depth and age. *Journal of Geophysical Research*, 95, 9153–9170.
- Cerney, B., & Carlson, R. L. (1999). The effect of cracks on the seismic velocities of Basalt from site 990, SE Greenland margin. *Proceeding of the Ocean Drilling Program, Scientific Results*, 163, 29–35.
- Chatterjee, N., & Bhattacharji, S. (2008). Trace elements variation in Deccan basalts: Role of mantle melting, fractional crystallization and crustal assimilation. *Journal of Geological Society of India*, 71, 171–188.
- Christensen, N. I. (1968). Compressional wave velocities in basic rocks. *Pacific Science*, XXII, 41–44.
- Christensen, N. I., Blair, S. C., Wilkens, R. H., & Salisbury, M. H. (1980). Compressional wave velocities, densities, and porosities of basalts from Holes 417A, 417 D, and 418 A. Deep Sea Drilling Project Legs 51–53. In: T. Donnelly et al. (Eds.), *Init. Reports DSDP*, 51, 52, 53 (part 2, pp. 1467–1471).
- Christensen, N. I., & Mooney, W. D. (1995). Seismic velocity structure and composition of the continental crust: A global view. *Journal of Geophysical Research*, 100, 9761–9788.
- Courtillot, V., Feraud, G., Maluski, H., Vandamme, D., Moreau, M. G., & Besse, J. (1988). Deccan flood basalts and the cretaceous/tertiary boundary. *Nature*, 333, 843–846.

- Cox, K. G., & Hawkesworth, C. J. (1985). Geochemical Stratigraphy of the Deccan Traps at Mahabaleshwar, Western Ghats, India, with implications for open system magmatic process. *Journal of Petrology*, 26, 355–377.
- Cox, K. G., & Mitchell, C. (1988). Importance of crystal settling in the differentiation of Deccan Trap basaltic magmas. *Nature*, 333, 447–449.
- Dixit, M. M., Tewari, H. C., & Visweswara Rao, C. (2010). Two-dimensional velocity model of the crust beneath the South Cambay Basin, India from refraction and wide-angle reflection data. *Geophysical Journal International*, 181, 635–652.
- Goldberg, D., & Sun, Y. F. (1997). Attenuation differences in layer 2A in intermediate- and slow-spreading oceanic crust. *Earth and Planetary Science Letters*, 150, 221–231.
- Goldberg, D., & Yin, C. S. (1994). Attenuation of p-waves in oceanic crust: Multiple scattering from observed heterogeneities. *Geophysical Research Letters*, 21, 2311–2314.
- Gradstein, F. M., Ogg, J. G., Schmitz, M. D., & Ogg, G. M. (2012). *The Geologic Time Scale 2012*. Amsterdam: Elsevier.
- Gupta, H. K., & Dwivedi, K. K. (1996). Drilling at Latur earthquake region exposes a peninsular gneiss basement. *Journal of Geological Society of India*, 47, 129–131.
- Gupta, H. K., & Gupta, G. D. (2003). Earthquake studies in Peninsular India since 1993. *Memoir Geological Society of India*, 54, 254.
- Gupta, H. K., Mohan, I., Rastogi, B. K., Rao, C. V. K., & Rao, G. V., et al. (1993). Investigation of Latur earthquakes of September 30, 1993. In: *Abstract Volume, Workshop on 30 September 1993 Maharashtra Earthquake, December 24, 1993*, Hyderabad, pp. 2–3
- Gupta, H. K., Srinivasan, R., Rao, R. U. M., Rao, G. V., Reddy, G. K., Roy, S., et al. (2003). Borehole investigations in the surface rupture zone of the 1993 Latur SCR earthquake, Maharashtra, India: Overview of results. *Memoir Geological Society of India*, 54, 1–22.
- Ivankina, T. I., Kern, H. M., & Nikitin, A. N. (2005). Directional dependence of P- and S-wave propagation and polarization in foliated rocks from Kola superdeep well: Evidence from laboratory measurements and calculations based on TOF neutron diffraction. *Tectonophysics*, 407, 25–42.
- Jay, A. E., & Widdowson, M. (2008). Stratigraphy, structure and volcanology of the SE Deccan continental flood basalt province: Implications for eruptive extent and volumes. *Journal Geological Society of London*, 165, 177–188.
- Ji, S., Wang, Q., & Salisbury, M. H. (2009). Composition and tectonic evolution of the Chinese continental crust constrained by Poissons' ratio. *Tectonophysics*, 463, 15–30.
- Kern, H., Megiel, K., Strauss, K. W., Ivankina, T. I., Nikitin, A. N., & Kukkonen, I. T. (2009). Elastic wave velocities, chemistry and modal mineralogy of crustal rocks sampled by the Outokumpu scientific drill hole: Evidence from lab measurements and modeling. *Physics of the Earth and Planetary Interiors*, 175, 151–166.
- Kern, H., Walther, C. H., Fluh, E. R., & Marker, M. (1993). Seismic properties of rocks exposed in the POLAR profile region—Constraints on the interpretation of the refraction data. *Precambrian Research*, 64, 169–187.
- Krishna, A. K., & Govil, P. K. (2007). Soil contamination due to heavy metals from an Industrial area of Surat, Gujarat, Western India. *Environmental Monitoring and Assessment*, 124, 263–275. <https://doi.org/10.1007/s10661-006-9224-7>.
- Lewis, B. T. R., & Jung, H. (1989). Attenuation of refracted seismic waves in young oceanic crust. *Bulletin of the Seismological Society of America*, 79, 1070–1088.
- Lightfoot, P. C., Hawkesworth, C. J., Devey, C. W., Rogers, N. W., & Van Calsteren, P. W. C. (1990). Source and differentiation of Deccan trap lavas: Implications of geochemical and mineral chemical variations. *Journal of Petrology*, 31, 1165–1200.
- Mahoney, J. J. (1988). Deccan traps. In J. D. Macdougall (Ed.), *Continental flood basalts* (pp. 151–194). Dordrecht: Kluwer Academic.
- Mitchell, C. H., & Widdowson, M. (1991). A geological map of the southern Deccan, India and its structural implications. *Journal of Geological Society of London*, 148, 495–505.
- Moose, D., & Zoback, M. D. (1983). In situ studies of velocity in fractured crystalline rock. *Journal of Geophysical Research*, 88(B3), 2345–2358.
- Murphy, W. F. (1982). Effects of partial water saturation on attenuation in Massilon sandstone and Vycor porous glass. *The Journal of the Acoustical Society of America*, 71(6), 1458–1468. <https://doi.org/10.1121/1.387843>.
- Murty, A. S. N., Koteswara Rao, P., Dixit, M. M., Kesava Rao, G., Reddy, M. S., Prasad, B. R., et al. (2011). Basement configuration of the Jhagadia-Rajpipla profile in the western part of Deccan syncline, India from travel-time inversion of seismic refraction and wide-angle reflection data. *Journal of Asian Earth Sciences*, 40, 40–51.
- Murty, A. S. N., Rajendra Prasad, B., Rao, Koteswara, Raju, S., & Sateesh, T. (2010). Delineation of subtrappean Mesozoic sediments in Deccan syncline, India, using travel-time inversion of seismic refraction and wide-angle reflection data. *Pure and Applied Geophysics*, 167, 233–251.
- Pandey, O. P. (2008). Deccan Trap volcanic eruption affected the Archean Dharwar craton of southern India: Seismic evidences. *Journal of Geological Society of India*, 72, 510–514.
- Pandey, O. P. (2009). Shallowing of mafic crust and seismic instability in the high velocity Indian shield. *Journal of Geological Society of India*, 74, 615–624.
- Pandey, O. P. (2016). Deep Scientific drilling results from Koyna and Killari earthquake regions reveal why Indian shield lithosphere is unusual, thin and warm. *Geoscience Frontiers*, 7, 851–858. <https://doi.org/10.1016/j.gsf.2015.08.010>.
- Pandey, O. P., Chandrakala, K., Parthasarathy, G., Reddy, P. R., & Koti Reddy, G. (2009). Upwarped high-velocity mafic crust, subsurface tectonics and causes of intraplate Latur-Killari (M 6.2) and Koyna (M 6.3) earthquakes, India—A comparative study. *Journal of Asian Earth Sciences*, 34, 781–795.
- Pandey, O. P., Tripathi, P., Parthasarathy, G., Rajagopalan, V., & Sreedhar, B. (2014). Geochemical and mineralogical studies of chlorine-rich amphibole and biotite from the 2.5 Ga mid-crustal basement beneath the 1993 Killari earthquake region, Maharashtra, India: Evidence for mantle metasomatism beneath the Deccan Traps. *Journal of Geological Society of India*, 83, 599–612.
- Pandey, O. P., Tripathi, P., Vedanti, M., & SrinivasaSarma, D. (2016). Anomalous seismic velocity drop in iron and biotite rich amphibolite to granulite facies transitional rocks from Deccan volcanic covered 1993 Killari earthquake region, Maharashtra (India): A case study. *Pure and Applied Geophysics*, 173, 2455–2471.

- Parthasarathy, G. (2006). Zeolite zonation and amygdaloidal minerals from the Killari borehole of Deccan traps, Maharashtra, India. *Journal of Applied Geochemistry*, 8, 546–557.
- Parthasarathy, G., Choudary, B. M., Sreedhar, B., Kunwar, A. C., & Srinivasan, R. (2003). Ferrous saponite from Deccan Trap, India, and its application in adsorption and reduction of hexavalent chromium. *American Mineralogist*, 88, 1983–1988.
- Prasanna Lakshmi, K. J., Senthil Kumar, P., Vijayakumar, K., Ravinder, S., Seshunrayana, T., & Sen, M. K. (2014). Petrophysical properties of the Deccan basalts exposed in the Western Ghats escarpment around Mahabaleshwar and Koyna, India. *Journal of Asian Earth Sciences*, 84, 176–187.
- Ramana, Y. V., & Rao, M. V. M. S. (1974). Q by pulse broadening in rocks under pressure. *Physics of the Earth and Planetary Interiors*, 8(4), 337–341. [https://doi.org/10.1016/0031-9201\(74\)90042-9](https://doi.org/10.1016/0031-9201(74)90042-9).
- Rao, M. V. M. S., & Prasanna Lakshmi, K. J. (2003). Shear-wave propagation in rocks and other lossy media: An experimental study. *Current Science*, 85, 1221–1225.
- Rao, M. V. M. S., Prasanna Lakshmi, K. J., Sarma, L. P., & Chary, K. B. (2006). Elastic properties of granulite facies rocks of Mahabalipuram, Tamil Nadu, India. *Journal of Earth System Science*, 115(6), 673–683. <https://doi.org/10.1007/s12040-006-0005-z>.
- Reddy, G. K., Rao, G. V., & Rao, R. U. M. (1998). Low density of Deccan traps: Evidence from boreholes at Killari, Latur earthquake site and implications for geophysical modeling. In: *Abstract volume, Chapman Conference on Stable Continental Region (SCR) earthquakes*, Hyderabad, 25–29 January, p. 31.
- Renne, P. R., Sprain, C. J., Richards, M. A., Self, S., Vandekruysen, L., & Pande, K. (2015). State shift in Deccan volcanism at the Cretaceous-Paleogene boundary, possibly induced by impact. *Science*, 350(Issue 6256), 76–78.
- Rudnick, R. L., & Fountain, D. M. (1995). Nature and composition of the continental crust: A lower crustal perspective. *Reviews of Geophysics*, 33, 267–309.
- Sano, T., Fujii, T., Deshmukh, S. S., Fukuoka, T., & Aramaki, S. (2001). Differentiation process of Deccan trap basalts: Contribution from geochemistry and experimental petrology. *Journal of Petrology*, 42, 2175–2195.
- Schoene, B., Samperton, K. M., Eddy, M. P., Keller, G., Adatte, T., et al. (2015). U-Pb geochronology of the Deccan Traps and relation to the end-Cretaceous mass extinction. *Science*, 347(6218), 182–184.
- Sen, G. (2001). Generation of Deccan trap magmas. *Proceedings of Indian Academy of Sciences (Earth Planet Sci.)*, 110, 409–431.
- Sen, G., Borges, M., & Marsh, B. D. (2006). A case for short duration of Deccan Trap eruption. *EOS*, 87(20), 197–204.
- Sen, G., & Chandrasekharam, D. (2011). Deccan trap flood basalt province: An evaluation of the thermochemical plume model. In: J. Ray, et al. (Eds.), *Topics in igneous petrology*. [https://doi.org/10.1007/978-90-481-9600-5\\_2](https://doi.org/10.1007/978-90-481-9600-5_2).
- Shrivastava, J. P., Duncan, R. A., & Kashyap, M. (2015). Post-K/PB younger  $^{40}\text{Ar}$ - $^{39}\text{Ar}$  ages of the Mandla lavas: Implications for the duration of the Deccan volcanism. *Lithos*, 224, 214–224.
- Shrivastava, J. P., Kumar, R., & Rani, N. (2017). Feeder and post Deccan Trap dyke activities in the northern slope of the Satpura Mountain: Evidence from new 40Ar-39Ar ages. *Geoscience Frontier*, 8, 483–492.
- Shrivastava, J. P., Mahoney, J. J., & Kashyap, M. R. (2014). Trace elemental and Nd-Sr-Pb isotopic compositional variation in 37 lava flows of the Mandla lobe and their chemical relation to the western Deccan stratigraphic succession, India. *Mineralogy and Petrology*, 108, 801–817.
- Sun, S., Ji, S., Wang, Q., Xu, Z., Salisbury, M., & Long, C. (2012). Seismic velocities and anisotropy of core samples from the Chinese continental scientific drilling borehole in the Sulu UHP terrane, Eastern China. *Journal of Geophysical Research*, 117, B01206. <https://doi.org/10.1029/2011JB008672>.
- Tisato, N., & Quintal, B. (2014). Laboratory measurements of seismic attenuation in sandstone: Strain versus fluid saturation effects. *Geophysics*, 79(5), WB9–WB14. <https://doi.org/10.1190/geo2013-0419.1>.
- Tompkins, M. J., & Christensen, N. I. (2001). Ultrasonic P-and S-wave attenuation in Oceanic Basalt. *Geophysical Journal International*, 145, 172–186.
- Tripathi, P. (2015). Nature and composition of crystalline basement below Deccan volcanic covered 1993 Latur-Killari earthquake region, Maharashtra (India). *Ph.D. thesis, Osmania University, Hyderabad, India*, p. 164.
- Tripathi, P., Pandey, O. P., Rao, M. V. M. S., & Koti Reddy, G. (2012a). Elastic properties of amphibolite and granulite facies mid-crustal basement rocks of the Deccan volcanic covered 1993 Latur-Killari earthquake region, Maharashtra (India) and mantle metasomatism. *Tectonophysics*, 554–557, 159–168.
- Tripathi, P., Parthasarathy, G., Masood Ahmed, S. M., & Pandey, O. P. (2012b). Mantle-derived fluids in the basement of the Deccan trap: Evidence from stable carbon and oxygen isotopes of carbonates from the Killari borehole basement, Maharashtra, India. *International Journal of Earth Sciences*, 101, 1385–1395.
- Ullemeyer, K., Nikolayev, D. I., Christensen, N. I., & Behrmann, J. H. (2011). Evaluation of Intrinsic velocity-pressure trends from low-pressure P-wave velocity measurements in rocks containing microcracks. *Geophysical Journal International*, 185, 1312–1320.
- Vedanti, N., Lakshmi, K. J. P., Dutta, S., Malkoti, A., & Pandey, O. P. (2015). Investigation of petrophysical properties and ultrasonic P-and S-wave attenuation in Deccan Flood Basalts, India. In: *SEG technical program expanded abstracts*, pp. 3274–3278. <https://doi.org/10.1190/segam2015-5858683.1>
- Vijaya Kumar, K., Chavan, C., Sawant, S., Naga Raju, K., et al. (2010). Geochemical investigation of a semi-continuous extrusive basaltic section from the Deccan volcanic province, India: Implications for the mantle and magma chamber processes. *Contributions to Mineralogy and Petrology*, 159, 839–862.
- Volarovitch, M. P., & Gurvitch, A. S. (1957). Investigation of dynamic moduli of elasticity for rocks in relation to temperature. *Bulletin Academy of Sciences, USSR Geophysics Series*, 4, 1–9.
- Walker, G. P. (1993). Basaltic-volcano systems. In: H. M. Richard, T. Alabaster, N. B. W. Harris, & C. R. Neary (Eds.), *Magmatic processes and plate tectonics* (pp. 3–38). Geological Society Special Publication no. 76.
- Weiner, A. T., Manghnani, M. H., & Raj, R. (1987). Internal friction in tholeiitic basalts. *Journal of Geophysics Research*, 92(11), 635–643.
- Wepfer, W. W. (1989). Application of laboratory velocities and attenuation data to the Earth's crust. *Ph.D. Thesis, Purdue University, West Lafayette, IN*.
- Wepfer, W. W., & Christensen, N. I. (1990). Compressional wave attenuation in oceanic basalts. *Journal of Geophysical Research*, 95, 431–439.

Wepfer, W. W., & Christensen, N. I. (1991). Q-structure of the oceanic crust. *Marine Geophysical Researches*, 13(3), 227–237.  
<https://doi.org/10.1007/BF00369151>.

White, D. J., & Clowes, R. M. (1994). Seismic attenuation structure beneath the Juan de Fuca ridge from tomographic inversion of amplitudes. *Journal of Geophysical Research*, 99, 3043–3056.  
Winkler, K. W., & Nur, A. (1982). Seismic attenuation: Effects of pore fluids and frictional sliding. *Geophysics*, 47, 1–15.

(Received September 13, 2017, revised February 21, 2018, accepted February 22, 2018)